What Drives Plate Motion?

Yongfeng Yang

Bureau of Water Resources of Shandong Province

No. 127, Lishan Road, Jinan, Shandong Province, 250014, CHINA

E-mail: roufeng_yang@yahoo.com, roufengyang@gmail.com

Abstract

Plate motion is an amazing feature on the Earth and is widely ascribed to several driving forces like ridge push, slab pull, and basal drag. However, an in-depth investigation shows these forces incomplete. Here we propose, the deep oceans are generating pressures everywhere, the application of these pressures over the walls of ocean basins, which consists of the sides of continents, may yield enormous horizontal forces (i.e., the ocean-generating forces), the net effect of these forces provides lateral push to the continents and may cause them to move horizontally, further, the moving continents drag the crusts that they connect to move, these totally give birth to plate motion. A roughly estimation shows that the ocean-generating forces may give South American, African, Indian, and Australian continents a movement of respectively 2.8, 4.2, 5.7, and 6.3 cm/yr, and give Pacific Plate a movement of 8.9 cm/yr.

1 Introduction

One of the most significantly achievements in the 20th century was the establishment of plate tectonics that developed from a previous conception of continental drift. The continent drift theory hypothesized that the continents had slowly floated over the Earth's surface in the distant past (Wegener, 1915 and 1924). The evidences supporting this surface motion include a shape fitting at the opposed sides of African and American continents, coal belt crossed

from North American to Eurasian, identical direction of ice sheet of southern Africa and India, and speed measurement made by global positioning system (GPS). In addition, the discovery of paleomagnetic reversals in oceans, which reflects seafloor spreading, further consolidated the belief of Earth's surface motion (Hess, 1962; Vine and Matthews, 1963). Nevertheless, the driving force behind this motion always remains poorly understood. The first to consider the dynamics source of this motion is the contraction theory, which proposed that a wrinkling process of Earth's surface had forced the Himalayas to climb up. Wegener (1915) ascribed continent's drift to the centrifugal and tidal forces, these forces were latterly found to be too weak to work. Jeffreys (1929) estimated that the mean tidal friction slowing the Earth's rotation corresponds to a westward stress of the order of only 10^{-4} dyn/cm^2 over the Earth's surface, this stress is too small to maintain that drift. After these attempts failed, people turned their eyes to the interior of the Earth to seek for the answer, together with the rebirth of the continental drift theory in the form of 'plate tectonics', they eventually fostered a series of driving forces like ridge push, slab pull, basal drag, slab suction, the geoid's deformation, and the Coriolis force (Holmes, 1931; Runcorn, 1962a, b; Turcotte and Oxburgh, 1972; Oxburgh and Turcotte, 1978; Spence, 1987; White & McKenzie, 1989; Conrad & Lithgow-Bertelloni, 2002). Of these driving forces, the geoid's deformation is almost symmetrical relative to the Earth's shape, the Coriolis force is also symmetrical relative to equator, these two forces can be easily excluded. Slab suction occurs when local mantle currents exert a downward pull on nearby plates in the subduction zone (McKenzie, 1969; Sleep & Toksoz, 1971; Elsasser, 1971; Richter, 1973), but its nature hasn't been well understood (Forsyth & Uyeda, 1975; Conrad & Lithgow-Bertelloni, 2002). Finally, ridge push, slab pull, and basal drag are thought to be the mostly driving forces for plate motion. A strictly investigation, however, reveal there are large uncertainties for these forces.

Ridge push is usually treated either as a body force or as a boundary force. As a body force, ridge push derives from the horizontal pressure gradient of the cooling and thickening of the oceanic lithosphere and acts over the area of the oceanic portion of a given plate (McKenzie, 1968; McKenzie, 1969; Richards, 1992; Vigny et al., 1992). Instead, as a boundary force, ridge push derives from a "gravity wedging" effect of warm, buoyant mantle upwelling beneath the ridge crest and acts at the edge of the lithospheric plate (Forsyth & Uyeda, 1975; Bott, 1993). Forsyth & Uyeda (1975) are the first to define ridge push as an edge force, from then on, it has been widely used as a boundary force to drive plate (Hager and O'Connell, 1981; Spence, 1987; White & McKenzie, 1989; Turcotte and Schubert, 2002; Turcotte and Schubert, 2014). There are two key points to discount ridge push. On the one hand, since all the plates are steadily moving over the Earth's surface, naturally, a plate in motion would depart from another plate. This department would result in a fracture between the two plates.

If the fracture is deep, it would allow magma to erupt and form Mid-Oceanic Ridge (MOR). In this respect, the MOR itself may be a result of plate motion. In fact, Wilson and Burke (1973) had pointed out that the ridges may have formed as a passive consequence of the plates moving apart. But now, the MOR are treated as a cause to yield force and further drive the plate. This goes to the notorious chicken-or-egg question, who is the first? In physical field, it is strictly required that a movement (i.e., result) must be separated from the force (i.e., cause) that sustains it. On the other hand, the measured tectonic stresses commonly showed that the stresses manifested by the lithosphere mainly concentrate on the uppermost brittle part of the lithosphere (Forsyth & Uyeda, 1975; Bott and Kusznir, 1984; Zoback & Magee, 1991; Wan, 2018). The region exerted by ridge push on the lithosphere is geographically lower, it is very difficult for ridge push to create a stress field crossing over the uppermost brittle crust. In the section of discussion of this work, we will further demonstrate how ridge push cannot be in accordance with the measured tectonic stresses.

Slab pull derives from a cold, dense sinking plate that uses its own weight to pull the remaining plate it attaches (Forsyth & Uyeda, 1975; Conrad and Lithgow-Bertelloni, 2002; Turcotte and Schubert, 2014). There are two points to discount this force. On the one hand, there was once a well-known debate between 1980's and 1990's on which force (ridge push or slab pull) is the primary driving force for plate motion. Most of geophysicists at the time accepted slab pull as the primary driving force (Forsyth & Uyeda, 1975; Turcotte and Schubet, 1982). They believed that tectonic stresses caused by ridge push, basal drag, and slab pull generally hold a magnitude of 20~30 MPa, and that at the front edge of a subducting plate the magnitude may reach up to 1000 MPa when the downgoing slab in the deep mantle becomes denser (yielding large negative buoyancy). However, the magnitude of this buoyancy could be seriously overestimated as the mantle in the deep is denser than the subducting slab (Wan, 2018). Some authors latterly evaluated more parameters (such as depth variation, subduction speed difference, thickness of slab, and so on) to conclude that the negative buoyancy is about 40~290 MPa (Zang and Ning, 1994). The current view is ridge push rather than slab pull is the primary driving force for plate motion. On the other hand, the chicken-or-egg question also occurs on slab pull. As all the plates are moving over the Earth's surface, the oceanic plates are geographically somehow lower than the continental plates, this difference of elevation makes the oceanic plates in motion easily subducted into the continental plates to form downgoing slabs. In this respect, the downgoing slabs themselves may be a result of plate motion. But nowadays, the downgoing slabs are treated as a cause to yield force to further drive the plate.

Basal drag derives from mantle dynamics and was thought to be caused by the viscous moving asthenosphere along the bottom of lithosphere (Holmes, 1931; Pekeris, 1935; Hales, 1936; Runcorn, 1962a, b; Turcotte and Oxburgh, 1972; Oxburgh and Turcotte, 1978; Tanimoto & Lay, 2000; Turcotte and Schubert, 2014; Bercovici, et al., 2015). There are three points to discount this force. First of all, mantle dynamics itself remains controversial (Siler et al., 1988; Davies and Richards, 1992; Lay, 1994; Ogawa, 2008; Turcotte and Schubert, 2014). The cells proposed by mantle dynamics to undertake the asthenospheric motion require a strong fitting to plate size. Seismic tomography showed that rising mantle material beneath ridges only extends down 200 to 400 km (Foulger, et al., 2001). This depth gives an upper limitation on the scale of the proposed cells. Most of plates (South American, North American, Eurasian, and Pacific, for instance), however, hold a width of generally more than thousands of kilometers, such width has been far beyond the scale of the proposed cells. Toroidal motion proposed by mantle dynamics was used to undertake horizontal rotation, but numerous studies of basic 3-D convection with temperature-dependent viscosity had failed to yield the requisite toroidal flow (Bercovic, 1993, 1995b; Cadek et al., 1993; Christensen and Harder, 1991; Tackley, 1998; Trompert and Hansen, 1998; Weinstein, 1998; Stein et al., 2004). In addition, mantle dynamics often envisages large convection to create a "conveyor belt" effect to entrain the lithosphere. The lithosphere moves at a speed of 0.1~12.0 cm per year, the horizontal speed of solid mantle inferred from hot spots was found to be less than 2.0 cm (Minster and Jordan, 1978), it is practically impossible for a slower mantle to entrain a faster lithosphere to move. Bott and Kusznir (1984) suggested that it is better for the lithosphere to entrain the upper mantle than for mantle convection to entrain the lithosphere. Second, a lack of correlation between plate velocity and surface area suggests that basal drag cannot be a driving force (Forsyth & Uyeda, 1975). Some authors argued that the contribution of basal drag to plate motion depends on the flow pattern at the lithosphere mantle interface (Doglioni, 1990), but the nature of this interface and its flow pattern are still unclear. So far, most of geophysicists believe basal friction to be resistive rather than driving (e.g., Richter, 1973; Richardson and Cox, 1984; Turcotte and Schubert, 2002; Turcotte and Schubert, 2014). Last, according to Zoback (1992), the predicted stresses related to whole mantle flow inferred from seismic tomography cannot match well with the broadest scale tectonic stress data.

During the past 50 years, we witnessed a great progress of plate tectonics. Plates were found to be periodically dispersed and aggregated in the mesozoic, companied with 5~6 significant astronomical events (Cande, et al., 1989; Cande and Kent, 1992; Ma, et al., 1996; Burchfiel, et al., Wan, 1993; Hibsch, et al., 1995). The speed and direction of plate motion supported by paleomagnetism and deformation in the intraplates exhibited various styles in the geological time (Wan, 2018). Tectonic stresses were globally measured and revealed strong correlation

between absolute or relative speed of plate motion and tectonic stresses, by which the forces acting on the plates may be constrained (Bott and Kusznir, 1984; Zoback et al., 1989; Zoback & Magee, 1991; Zoback, 1992; Richards, 1992; Sperner et al., 2003; Heidbach et al., 2007; Heidbach et al., 2010; Heidbach et al., 2016; Heidbach et al., 2018; Wan, 2018). In particular, mantle dynamics was refreshed with the conceptions of plume and surge (Wilson, 1963; Condie, 2001; Meyerhoff, 1996; Torsvik, et al., 2008; Domeier and Torsvik, 2014). With the development of plate tectonics, the exploration of the plate driving force keeps ongoing (Conrad and Lithgow-Bertelloni, 2004; Faccenna, et al., 2012; Eagles and Wibisono, 2013; Turcotte and Schubert, 2014; Bercovici, et al., 2015; Mallard, et al., 2016; Crameri, et al., 2018). Since 1970's, some authors had begun to evaluate the relative importance of these driving forces (Forsyth & Uyeda, 1975; Backus, et al., 1981; Bokelmann, 2002). These efforts give people a sense that all the forces related to plate motion had been found. The fact, however, is not so, a significant force has been completely ignored. In this work, we get back to the exterior of the Earth to seek for this force and very hopefully expand our understanding of plate motion.

2 An ocean-generating force driving mechanism for plate motion

2.1 Forces acting on continent

Liquid can exert pressure at the wall of a container that holds it. According to Figure 1, the pressure generated at the wall of a cubic container may be written as $P=\rho g y/2$, the application of this pressure over the wall yields a horizontal force, this force may be expressed as $F=PS=\rho g y^2 x/2$, where S is the wall's area, ρ and g are respectively the liquid's density and gravitational acceleration, x and y are respectively the liquid's width and depth in the container. Get back to real world, ocean basins are naturally gigantic containers, their depths are often more than a few kilometers and especially vary from one place to another. All these determine that oceans can generate enormous pressures everywhere and the pressures generated are unequal between oceans, furthermore, the application of these pressures over the ocean basins' walls, which consist of the continent's sides, can yield enormous unequal forces for the continents. Geometrically, ocean pressure exerts always vertical to the continental slope, by which a normal force is formed. This normal force will be called ocean-generating force. This force can be further decomposed into a horizontal force and a vertical force. We here define the continental crust, which can be applied by ocean pressure, as continent in the following sections. Subsequently, we list the plausible forces acting on the continent as illustrated in Figure 1 and discuss the physical nature of these forces. The forces acting on continents can be classified into two categories: the forces acting at the parts of

continent that connect to ocean, and those acting at both the bottom surface of continent and the parts of continent that connect to adjacent crusts. The forces acting at the parts of continent that connect to ocean derive from ocean pressures. They are the ocean-generating forces and denoted F_R at the right and F_L at the left. The horizontal forces decomposed from these forces are denoted F_R' at the right and F_L' at the left. The force acting at the bottom surface of continent arises from a viscous coupling between the continent and underlying asthenosphere. It will be called basal friction force and denoted f_{base}. As addressed by Forsyth & Uyeda (1975), if there is an active flow in the asthenosphere, such as thermal convection, f_{base} will act as a driving force (Runcorn, 1962a, b; Morgan, 1972; Turcotte & Oxburgh, 1972). If, on the other hand, the asthenosphere is passive with regard to the plate motion, f_{base} will be a resistive force. We here assume f_{base} to be a resistive force. The forces acting at the parts of continent that connect to adjacent crusts arise from a physical binding of the continent and adjacent crusts, given the continent moves towards right, they will be called push force from the crust at the right side, pull force from the crust at the left side, shearing force from the crust at the far side, and shearing force from the crust at the near side, and denoted f_{right}, f_{left}, f_{far}, and f_{near}, respectively. It is important to note that, if there were no fractures (i.e., the gaps along ocean ridges) within ocean basin, the ocean-generating forces may be balanced out by the basin itself. Forsyth & Uyeda (1975) showed that the world's extensional boundaries represented by the fractures may reach up to 50,000 km. The fractures in the ocean basins allow the ocean-generating forces to interact with the basal friction. And then, a combination of all these forces for the continent in the horizontal direction may be written as

$$F = (F_L' - F_R') - (f_{base} + f_{right} + f_{left} + f_{far} + f_{near}) \qquad (1)$$

where the first term $(F_L' - F_R')$ denotes the net horizontal force, which provides a dynamic source for the continent, the second term $(f_{base} + f_{right} + f_{left} + f_{far} + f_{near})$ denotes the total resistive force, which attempts to hinder the continent's movement. We here mark $(F_L' - F_R')$ with $F_{horizontal}$, and mark $(f_{base} + f_{right} + f_{left} + f_{far} + f_{near})$ with $F_{resistive}$. F_L' and F_R' may be further written as $F_L' = 0.5\rho g L h_L^2$, $F_R' = 0.5\rho g L h_R^2$, and ρ, g, L, h_L, and h_R are respectively density of water, gravitational acceleration, ocean's width that fits to the continent's width, ocean's depth at the left, and ocean's depth at the right.
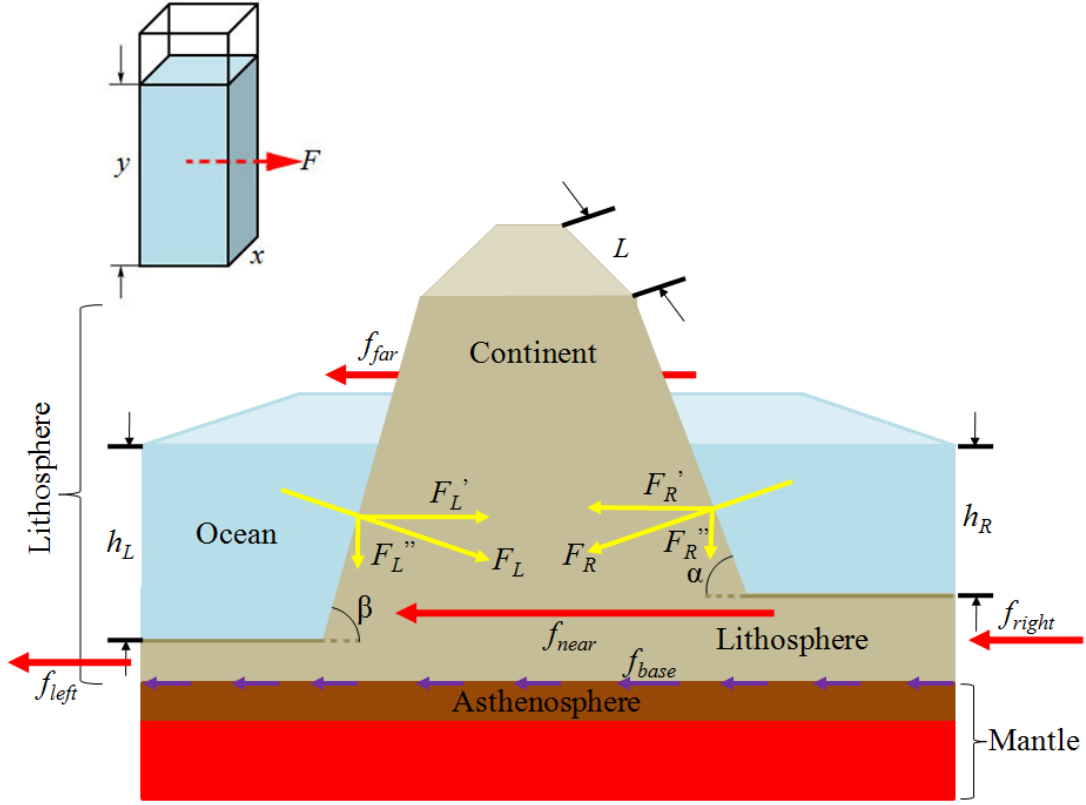
Fig. 1. Modelling the dynamics of continent. $F_L(F_R)$ represents the ocean-generating force at the left (right) side of the continent, while $F_L'(F_R')$ and $F_L''(F_R'')$ denote respectively the horizontal and vertical forces decomposed from the ocean-generating force. f_{base} denotes basal friction force exerted by the asthenosphere, while f_{right}, f_{left}, f_{far}, and f_{near} denote the push force from the crust at the right side, the pull force from the crust at the left side, the shearing force from the crust at the far side, and the shearing force from the crust at the near side of the continent. The continent is assumed to move towards left. L denotes the width of the continent's side, h_L and h_R are respectively ocean's depth at the left and at the right. α and β denote the inclinations of the continent's slope at both sides. Note that ocean depth is highly exaggerated with respect to the lithospheric thickness.

2.2 Continent's movement

Equation (1) above provides three possibilities for the continent. If the net horizontal force is always less than or equal to the total resistive force, the combined force will be less than or equal to zero, the continent would remain motionless; If the net horizontal force is always greater than the total resistive force, the combined force will be greater than zero, the continent would get an accelerating movement. Practically, it is impossible for the continent to own such a movement; And if the net horizontal force is sometimes greater than the total resistive force but other times less than the total resistive force, the combined force will be

discontinuous, the continent would get a discontinuous movement. We assume there exists a weak balance between the net horizontal force and the total resistive force, and this balance can be periodically broken by an unusual event. The existence of this weak balance would be discussed later. Most of oceans experience two cycles of high and low water per day, these movements of water are the tides we know in everyday life. The addition of tides to oceans makes oceans oscillate vertically, this leads the pressures in the oceans to periodically vary. Ocean pressure variations had been confirmed by bottom pressure measurements (Fig. 2). In particular, these variations exhibit different from one ocean to another during a month. For example, at the time of new Moon the range of bottom pressure variation at North Santo Domingo (Atlantic ocean) is almost within 100 millibars, while at South Dutch Harbor (Pacific ocean) the range may reach up to 260 millibars. The periodically varying pressures determine the net horizontal force generated to periodically vary, and thus provide possibility for the net horizontal force to be discontinuously greater and less than the total resistive force. And then, the continent's movement may be outlined with Figure 3: at the stage of t_1, the net horizontal force begins to increase, but since $F_{horizontal} - F_{resistive} < 0$, the continent remains motionless; At the stage of t_2, $F_{horizontal} - F_{resistive} > 0$, the continent is accelerated to move, and its speed reaches a highest level at the end of this period; At the stage of t_3, $F_{horizontal} - F_{resistive} < 0$, the continent begins to decelerate until its speed becomes zero at the end of this period; At the stage of t_4, due to $F_{horizontal} - F_{resistive} < 0$, the continent remains motionless; And at the stage of t_5 and t_6, the continent gets a movement that is similar to the movement at the stage of t_2 and t_3, but at the stage of t_7, the continent again remains motionless. Simply, the continent discontinuously obtains some forward movements at the stages of t_2, t_3, t_5, and t_6, and some stagnations at the stages of t_1, t_4, and t_7. These movements and stagnations totally provide a net forward movement for the continent during the day. Expanding this day to one year, the continent obtains a steadily forward movement during the year. Further, extending this year to a long timescale of millions of years and taking into account the matter that the oceans are extensively distributed around the globe, we conclude, the continents could have obtained steadily forward movements over millions of years. Figure 4 exhibits a globally distribution of the oceans and the resultant horizontal forces around the continents.
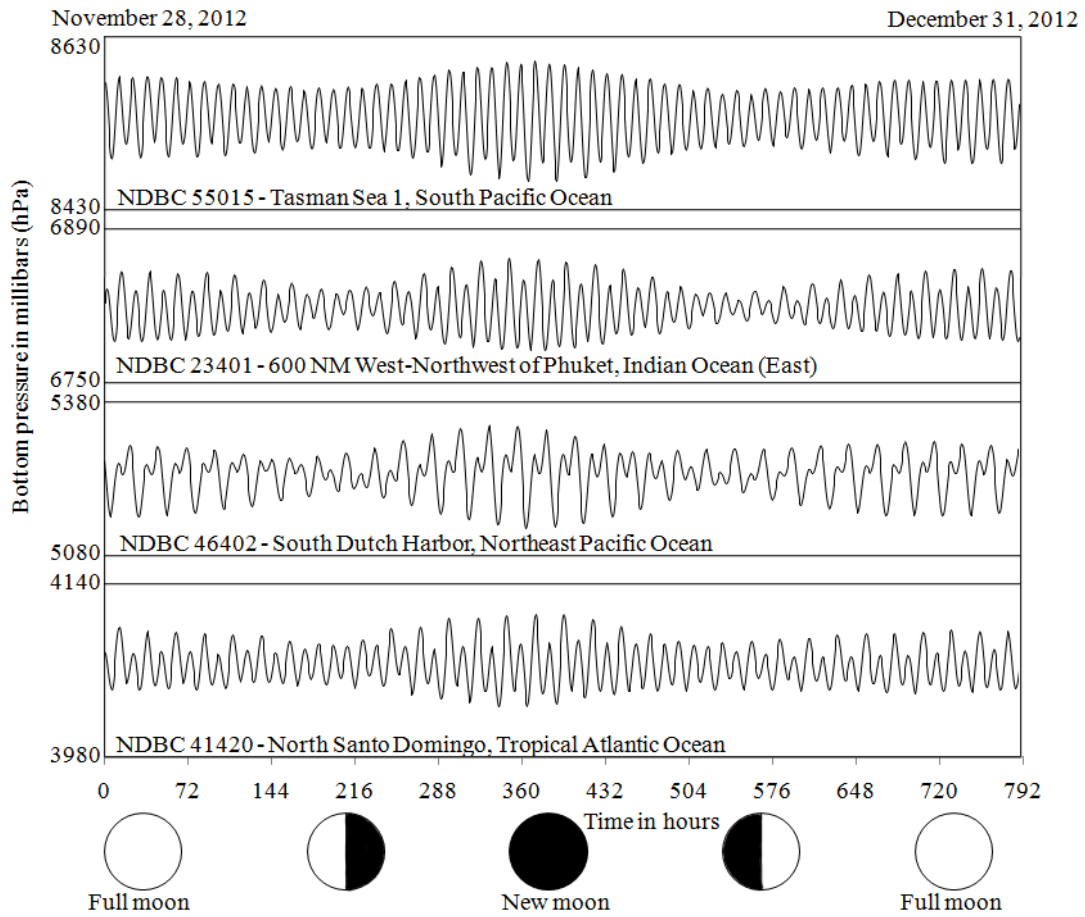
Fig. 2. Representatives of typical 1-month bottom pressure records during 2012. Bottom pressure record data are from PSMSL (Permanent Service for Mean Sea Level).
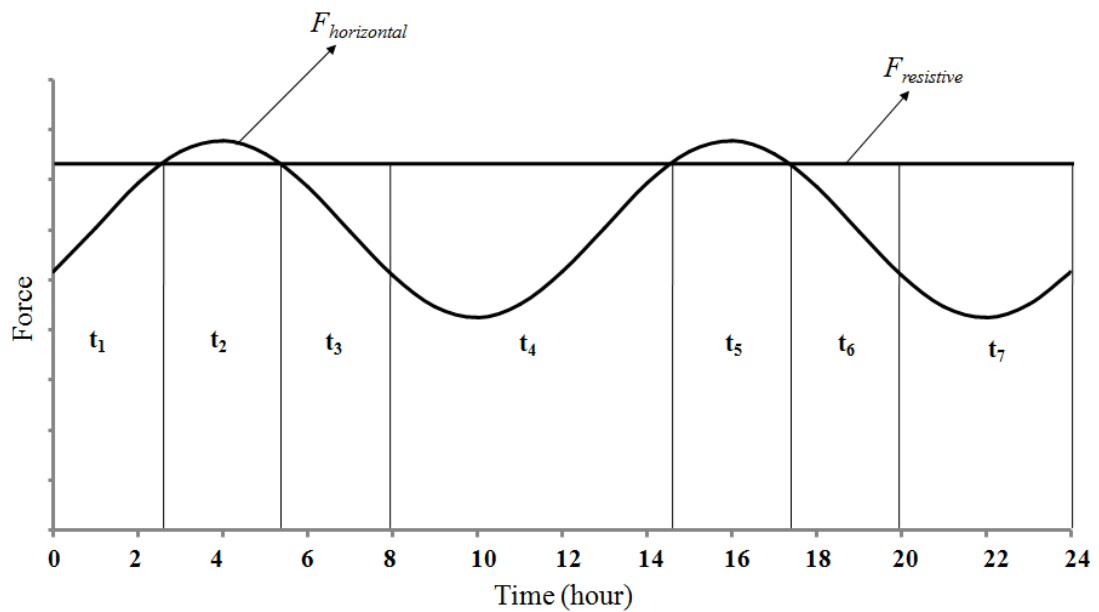

Fig. 3. Dynamic analysis for continent. $F_{horizontal}$ denote the net horizontal force generated for the

continent, $F_{resistive}$ denotes the total resistive force undergone by the continent. Note that the oscillation of the net horizontal force is somehow exaggerated.
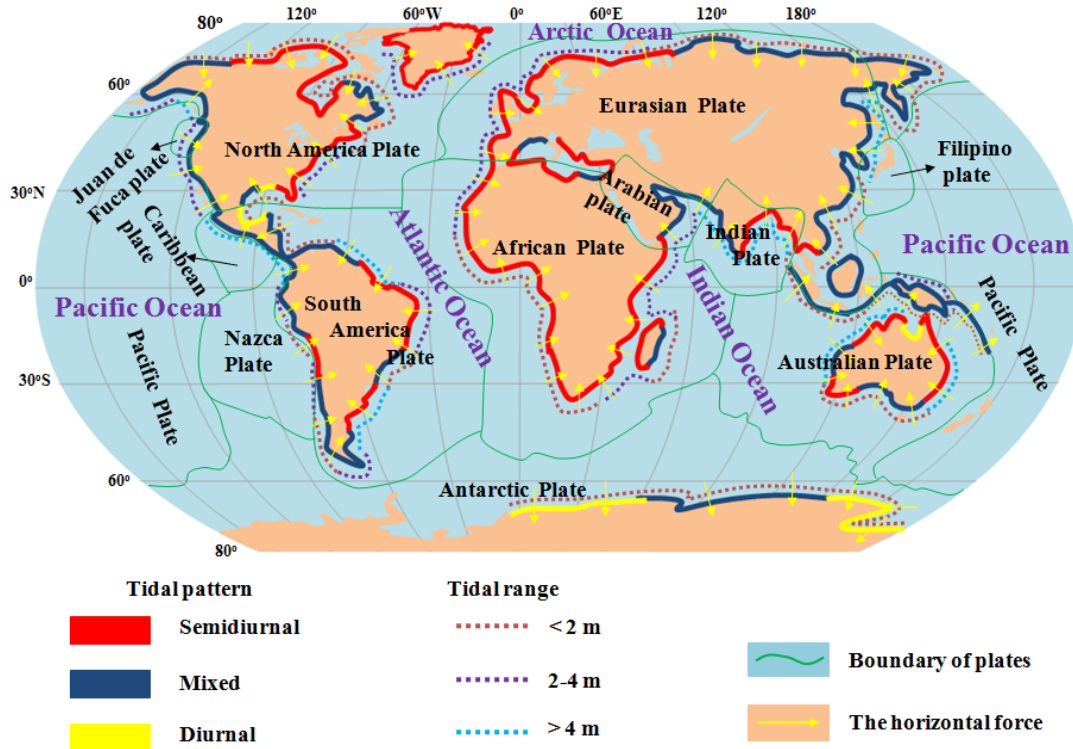

Fig. 4. A global view of the distribution of tidal pattern, tidal range, plate tectonics, and the horizontal forces generated for continents. Tide data supporting is from U.S. NOAA, GLOSS database - University of Hawaii Sea Level Center (Caldwell et al. 2015), and Bureau National Operations Centre (BNOC) of Australia, and tide range also refer to the times atlas of the oceans, 1983, Van Nostrand Reinhold, NY.

A quantitative resolution of the continent's movement must consider more details. Most of continents are being surrounded by oceans, this indicates that the net horizontal force obtained by a continent would be a consequence of the combination of the horizontal forces generated at all the sides of this continent. The curved Earth's surface makes the horizontal forces generated unable to fall into a plane where they interact with each other. Additionally, the tides surrounding a continent are not synchronous, their amplitudes perform two cycles per month, this rhythm is thought to be related to the positions of the Sun, Moon, and Earth. For example, the tides become maximal at the times of full and new Moon, and become minimum at the times of first quarter and last quarter. Furthermore, the tidal loading/unloading rate is not uniform. More features of the tides may refer to these works (Pugh 1987; Pugh and Woodworth 2014). To realize our deduction smoothly, the continent is considered to be more rigid and its surface is assumed to be flat, this allows Newton's mechanics to be applicable. We further assume the tides around a continent to be synchronous and their amplitudes to be

10

constant during a month. The tidal loading/unloading rate is assumed to be linear, this enables us to easily infer that the time taken by the continent to accelerate is the same as the time taken to decelerate, namely, $t_2 = t_3$. And then, according to the knowledge of Newton's 2nd law, and given there are two tides per day, the movement that a continent obtains during a year may be approximately written as

$$D = \mathbf{365} * \mathbf{2} * \frac{1}{2} * \frac{(F_{horizontal-\max} - F_{resistive})}{M} * t^2 \qquad (2)$$

where $F_{horizontal\text{-}max}$ denotes the net horizontal force generated at the time of highest tide, $F_{resistive}$ denotes the total resistive force, M denotes the continent's mass and may be got through $M = Sd\rho_{continent}$ (where S, d, and $\rho_{continent}$ are respectively the continent's area, thickness, and density), t is the time that the continent takes to accelerate during a tide. As the horizontal forces exerted to the continent are often along different directions, we need to combine these forces into a final horizontal force. A strategy is to firstly decompose each of the horizontal forces into a latitudinal component and a longitudinal component, subsequently, by a simple addition, all the latitudinal and longitudinal components are separately combined into a latitudinal force and a longitudinal force, further, the latitudinal force and the longitudinal force are combined into a final horizontal force. The net horizontal force may be written as

$$F_{horizontal-\max} = \left((\sum_{i=1}^{n} F_{i-horizontal-latitudinal})^2 + (\sum_{i=1}^{n} F_{i-horizontal-longitudinal})^2 \right)^{\frac{1}{2}}, \quad \text{where} \quad F_{i\text{-}horizontal\text{-}latitudinal} \quad \text{and}$$

$F_{i\text{-}horizontal\text{-}longitudinal}$ are respectively the latitudinal and longitudinal components that are decomposed from the horizontal force, these components can be further expressed as $F_{i-horizontal-latitudinal} = F_{i-horizontal} \sin\Omega_i$, $F_{i-horizontal-longitudinal} = F_{i-horizontal} \cos\Omega_i$. Ω_i denotes the inclination of the ith side to latitude (+), and may be got through geographic latitudes and longitudes of the two ends of this side. $F_{i\text{-}horizontal}$ denotes the horizontal force generated at the ith side of the continent at the time of highest tide, and can be written as $F_{i\text{-}horizontal} = 0.5\rho gL(h_{ocean}+h_{tide})^2$. ρ, g, L, h_{ocean}, and h_{tide} are respectively density of water, gravitational acceleration, the continent side's width, the ocean depth that connects to the continent side, and tidal height. Tidal height may be expressed as $h_{tide}=A\sin\omega t$, A is tidal amplitude, ω and t are respectively angular frequency and time.

Practically, the continent's side is not flat, and the continent's base is generally wider than its top, these make the continent look more like a circular truncated cone staying in the ocean. As the horizontal force generated relates to the ocean's width (i.e., the continent side's width), we need to horizontally project the continent into a polygonal column and cut the whole side of

this column into a series of smaller rectangular sides connecting one to another, subsequently, to calculate the horizontal force generated at each of these rectangular sides, finally, we combine these horizontal forces to form a single horizontal force. With these theoretical ideas, we take the parameters involved to estimate the movements of a few continents (South American, African, Indian, and Australian). The controlling sites used to determine the length of side refer to Figure 5, the longitudes and latitudes of these sites are got through Google Earth software. The parameters involved and the horizontal forces generated are separately listed in Table 1 and 2. Please note, the determination of the time taken by the continent to accelerate and the time taken to decelerate during a tide is rather complicated. Mathematically, if these parameters such as tidal height, ocean depth, ocean width, and total resistive force can be given, we may refer Figure 3 to develop a non-linear relationship resolve the time. As we are attempting to estimate the continent's movement, the non-linear relationship is currently not considered, instead, we need to value the time. Finally, South American, African, Indian, and Australian continents obtain a movement of respectively 2.8, 4.2, 5.7, and 6.3 cm/yr, as shown in Table 3. These results are well consistent with the observed movement of generally 5.0~10.0 cm/yr (Read and Watson 1975).

Careful readers would discern that the total resistive force ($F_{resistive}$) we use in the calculation is technically valued. Undoubtedly, this treatment should deserve a discussion of necessity. As shown in Figure 1, the total resistive force includes four components: the basal friction force, the push force, the pull force, and the shearing forces. The push force, the pull force, and the shearing forces essentially originate from the basal frictions exerted by the asthenosphere onto the lithosphere. The basal friction is determined by a few factors, i.e., the asthenosphere's viscosity, the continent's area, the continent's speed, and the asthenosphere's thickness. The area and speed can be exactly measured, but the viscosity and thickness of the asthenosphere remain high uncertainty. Cathless (1971) concluded the viscosity no less than 10^{20} P, Jordan (1974) treated the thickness as 300 km. Fjeldskaar (1994) suggested that the asthenosphere has a thickness of less than 150 km and a viscosity of less than $7.0*10^{20}$ P. Some works using glacial isostatic adjustment and geoid studies concluded the asthenospheric viscosity ranges from 10^{19} to 10^{21} P (Hager and Richards, 1989; King, 1995; Mitrovica, 1996). James et al. (2009) used model to show that the asthenospheric viscosity is varied from $3*10^{19}$ P for a thin (140 km) asthenosphere to $4*10^{20}$ P for a thick (380 km) asthenosphere. These totally determine that the total resistive force cannot be exactly known and need to be valued.

Careful readers would also find that our understanding of the continent's movement relies on an assumption that there is a weak balance between the net horizontal force and the total resistive force. This balance should also deserve a discussion of possibility. The basal friction

exerted by the asthenosphere along the continent's base can be expressed as $F_A=\mu Au/y$, where μ, A, u, and y are respectively the viscosity of the asthenosphere, the continent's area, the continent's speed, and the thickness of the asthenosphere. We here adapt $\mu= 3*10^{19}$ P and $y=200$ km to estimate the basal friction forces undergone by the four continents (South American, African, Indian, and Australian). The speeds of these continents are assumed to be 2.7, 4.2, 5.6, and 6.4 cm/yr, respectively, and the areas of these continents are listed in Table 1. The basal friction forces estimated are eventually listed in Table 2. It can be found that, for each of these four continents, the magnitude of the horizontal force generated is extremely close to the magnitude of basal friction force. We believe this approach is not a coincidence, because these two forces are got through two different passages. Finally, we get to the point that there may be a weak balance between the net horizontal force and the total resistive force.
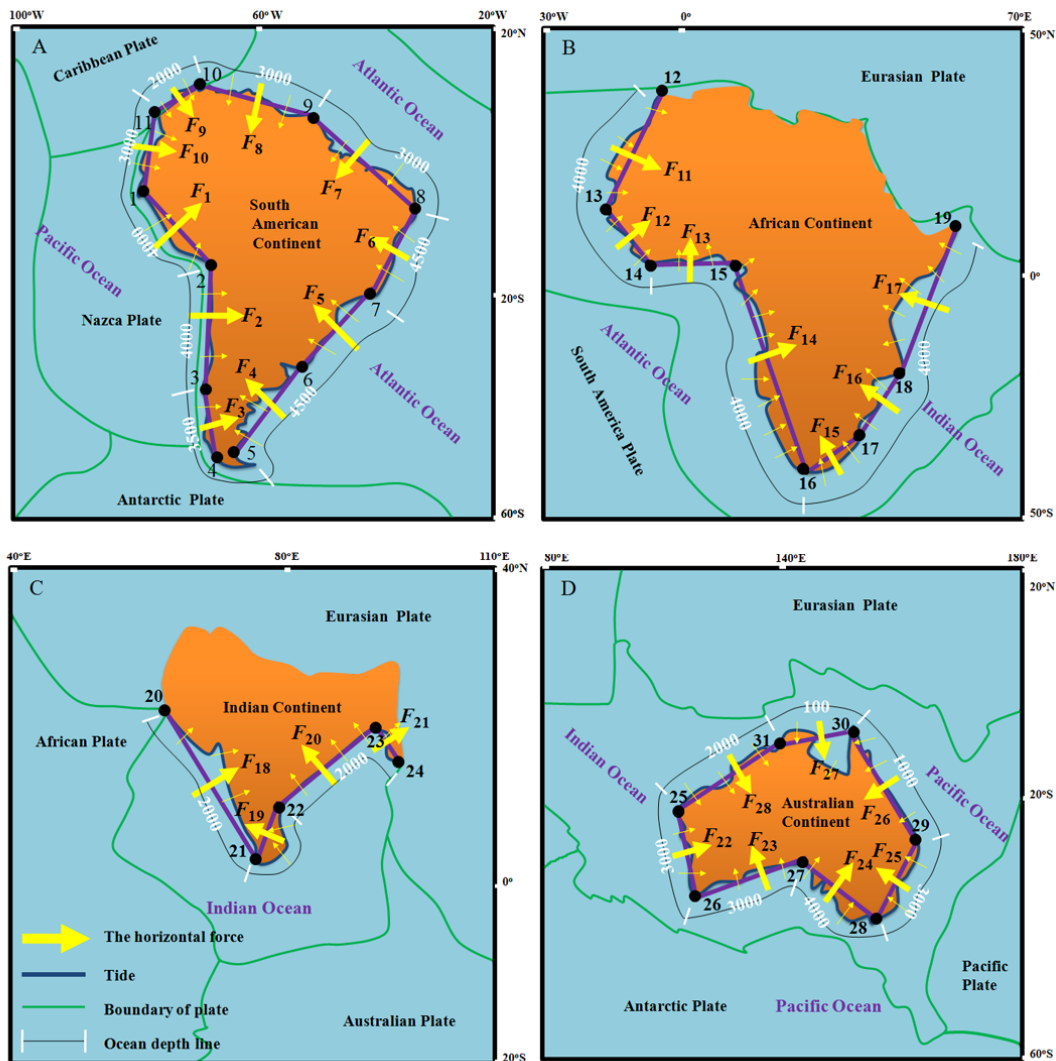
Fig. 5. Geographic treatment of the controlling sites for selected four continents and the horizontal forces generated for them. *F* (yellow arrow) denotes the horizontal force generated, while purple bar denotes the distance applied by the horizontal force. The product of this distance and ocean depth is the area applied by the horizontal force. Dot with number denotes controlling site. Ocean depth is artificially resolved from Google Earth software.

Table 1 Basic information for selected four continents

Continent	area	thickness	density	mass	site			site to site				tidal height	Ocean depth
								distance		inclination to latitude, east (+)			
	S	d	ρ	M				L		i	Ω_i	h_{tide}	h_{ocean}
	km^2	km	kg/m^3	kg	No.	Longitude	Latitude	km			degree (^{o})	m	m
South American	17,840,000	6	3,100	3.32E+20	1	80.0^{o}W	2.0^{o}S	1_2	2,087	1	122.01	1.5	4,000
					2	70.0^{o}W	18.0^{o}S	2_3	1,153	2	73.30	1.5	4,000
					3	73.0^{o}W	28.0^{o}S	3_4	2,780	3	90.00	1.5	3,500
					4	73.0^{o}W	53.0^{o}S	5_6	2,308	4	51.15	2.0	4,500
					5	68.0^{o}W	52.5^{o}S	6_7	1,730	5	43.78	2.0	4,500
					6	54.0^{o}W	34.5^{o}S	7_8	1,952	6	64.89	1.5	4,500
					7	42.0^{o}W	23.0^{o}S	8_9	2,525	7	146.66	1.5	3,000
					8	34.0^{o}W	7.0^{o}S	9_10	2,157	8	160.64	1.5	3,000
					9	53.0^{o}W	5.5^{o}N	10_11	836	9	41.26	1.5	2,000
					10	72.0^{o}W	12.0^{o}N	11_1	1,033	10	75.66	1.5	3,000
					11	78.0^{o}W	7.0^{o}N						
African	30,370,000	6	3,100	5.65E+20	12	6.0^{o}W	35.5^{o}N						
					13	17.0^{o}W	14.7^{o}N	12_13	2,535	11	117.65	1.0	4,000
					14	7.0^{o}W	4.6^{o}N	13_14	1,531	12	45.00	1.0	4,000
					15	8.0^{o}E	4.4^{o}N	14_15	1,696	13	3.81	1.0	4,000
					16	22.2^{o}E	34.7^{o}S	15_16	4,577	14	109.75	1.0	4,000
					17	30.4^{o}E	30.7^{o}S	16_17	886	15	26.00	1.0	4,000
					18	40.0^{o}E	16.0^{o}S	17_18	1,904	16	56.85	1.0	4,000
					19	51.0^{o}E	11.0^{o}N	18_19	3,237	17	67.83	1.0	4,000
Indian	4,400,000	6	3,100	8.18E+19	20	66.8^{o}E	25.0^{o}N						
					21	77.5^{o}E	8.0^{o}N	20_21	2,205	18	122.19	2.0	3,000
					22	80.0^{o}E	15.2^{o}N	21_22	846	19	70.85	2.0	3,000
					23	91.5^{o}E	22.7^{o}N	22_23	1,468	20	33.11	2.0	3,000
					24	94.3^{o}E	16.0^{o}N	23_24	801	21	112.68	2.0	3,000

					25	114.0^{o}E	23.0^{o}S	25_31	2,162	28	32.43	2.0	2,000
					26	117.2^{o}E	35.0^{o}S	25_26	1,370	22	104.93	2.0	4,000
					27	131.0^{o}E	31.5^{o}S	26_27	1,340	23	14.23	1.0	5,000
Australian	8,600,000	6	3,100	1.60E+20	28	149.8^{o}E	37.6^{o}S	27_28	1,846	24	162.02	1.0	5,000
					29	153.0^{o}E	25.4^{o}S	28_29	1,390	25	75.30	2.0	3,000
					30	142.4^{o}E	10.8^{o}S	29_30	1,970	26	125.98	2.0	1,000
					31	131.0^{o}E	12.2^{o}S	30_31	1,252	27	7.00	2.0	100

Note: all geographic sites refer to Figure 5; tidal height is half of tidal range.

Table2 The generated horizontal force and constrained parameters for selected four continents

Continent	i	the horizontal force [a]			$F_{horizontal\text{-}max}$	the resistive force [b] $F_{resistive}$	the friction [c] f_{base}	the time taken to accelerate during a tide [d] t
		horizontal	decomposed					
			latitudinal, east (+)	longitudinal, north(+)				
		$F_{i\text{-}horizontal}$	$F_{i\text{-}horizontal\text{-}latitudinal}$	$F_{i\text{-}horizontal\text{-}latitudinal}$				
		N(*10^{17})				N(*10^{17})		Second
South American	1	1.6375	1.3886	0.8679				
	2	0.9050	0.8668	-0.2600				
	3	1.6701	1.6701	0.0000				
	4	2.2925	-1.7853	1.4382				
	5	1.7184	-1.1890	1.2406				
	6	1.9378	-1.7546	0.8225				
	7	1.1148	-0.6127	-0.9313				
	8	0.9520	-0.3156	-0.8981				
	9	0.1642	0.1083	-0.1234				
	10	0.4559	0.4417	-0.1129				
			-1.1817	2.0434	2.3605	2.3604	2.2911	197.18
African	11	1.9883	1.7613	-0.9226				
	12	1.2006	0.8489	0.8489				
	13	1.3304	0.0885	1.3275				

	14	3.5900	3.3789	1.2129			
	15	0.6953	-0.3048	0.6249			
	16	1.4932	-1.2502	0.8164			
	17	2.5392	-2.3515	0.9580			
			2.1711	4.8662	5.3285	5.3283	6.0670	165.14
	18	0.9737	0.8241	0.5187			
	19	0.3734	-0.3527	0.1225			
Indian	20	0.6482	-0.3541	0.5430			
	21	0.3536	0.3263	0.1363			
			0.4435	1.3205	1.3930	1.3929	1.1720	144.59
	22	1.0751	1.0388	0.2770			
	23	1.6417	-0.4036	1.5914			
	24	2.2627	0.6983	2.1523			
	25	0.6137	-0.5936	0.1557			
Australian	26	0.0969	-0.0784	-0.0569			
	27	0.0006	0.0001	-0.0006			
	28	0.4246	0.2277	-0.3584			
			0.8892	3.7604	3.8641	3.8640	2.5771	175.62

Note: all horizontal forces generated refer to Figure 5;

a (the horizontal force) and c (the basal friction) are calculated, while b (the total resistive force) and d (the time taken to accelerate during a tide) are technically valued.

Table 3 The resultant movements for selected four continents

Continent	movement per year	to latitudinal direction, east (+)
	mm/yr	degree
South American	27.59	120.04
African	41.85	65.96
Indian	56.46	71.44
Australian	63.09	76.70

The treatment of the continent's movement above is relatively idealized. As most of the horizontal forces exerted on a continent are along different directions and cannot pass the barycenter of this continent, a torque effect may be created to rotate the continent. Figure 6 (A and B) conceptually demonstrates how these continents (Eurasian and North America, for instance) move under the torque effect yielded by the horizontal forces.
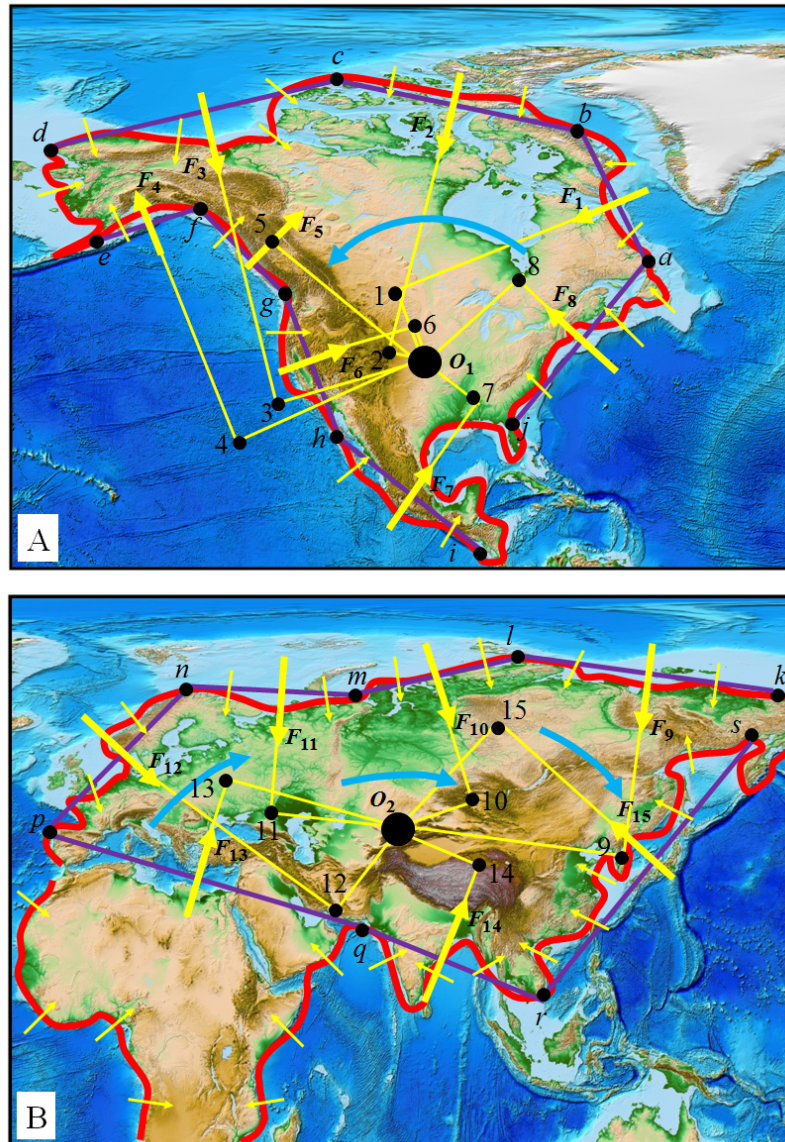
Fig. 6. Dynamics for the rotations of North American and Eurasian continents. O_1 and O_2 denote possible positions of the barycenters of two continents. F_1, F_2, F_3, i.e., marked with yellow arrows, denote the horizontal forces generated, *a, b, c,* i.e., denote the selected controlling sites, while *ab, bc, cd,* i.e., marked with purple bars, denote the length of continent's side, while $O_1 1$, $O_1 2$, . . ., $O_2 9$, $O_2 10$, i.e., denote the arms applied by the horizontal forces. Torque effect is expressed with a product of force and arm. Curved blue arrows represent expected rotations around these barycenters. Note F_{13} represents a lateral push force from the travelling African

20

continent. The background map is got from ETOPO1 Global Relief Model (Amante and Eakins, 2009).

2.3 Plate motion

Plate motion may be a consequence of the horizontal force. Refer to Figure 1 and Table 2, the majority of the net horizontal force has been used to oppose the total resistive force, which is composed of the basal friction exerted by the asthenosphere, the push force from the crust at the right side, the pull force from the crust at the left side, the shearing force from the crust at the far side, and the shearing force from the crust at the near side. By the principle of action and reaction, these resistive forces may further drive the crusts that bear them to move. We believe, it is such an interactive process to finally create plate motion over the globe.

Force transition from one plate to another may be expressed with Pacific Plate's motion. As outlined in Figure 7, Australian Plate and North American Plate independently provide push force F_{PA} and F_{PN} to Pacific Plate, a composition of these two forces would be the force F_P, which provides a dynamics for Pacific Plate. A quantitative treatment on Pacific Plate's motion is relatively complicated. Pacific Plate is firstly considered to be more rigid and plat. These assumptions allow deformation to be negligible and related forces to interact at a plane. According to a relationship of movement and force, equation (2) can be simplified as $F \sim DM$, where F, M, and D are respectively the force that a continent obtains, the continent's mass, and the continent's movement. Applying this simplified equation to South American continent, it would be $F_S \sim D_S M_S$. Furthermore, we apply this equation to North American continent and make analogy with South American continent, there would be $F_N \sim F_S D_N M_N / D_S M_S$, where F_N and F_S denote the net horizontal force obtained respectively by North American continent and South American continent, D_N and D_S are the movements obtained respectively by these two continents, M_N and M_S denote the masses of these continents. Refer to the parameters listed in Table 1, 2, and 3, there would be $F_S=2.3605*10^{17}$ N, $D_S=2.7$ cm per year, $M_S=3.32*10^{20}$ kg. North American continent has an area of about $24,709,000$ km^2, according to another expression $M=Sd\rho_{continent}$ (where S, d, and $\rho_{continent}$ are respectively the continent's area, thickness, and density), the continent's mass can be calculated as $M_N=4.60*10^{20}$ kg. North American Plate rotates counterclockwise and moves at a speed of about 1.5~2.5 cm per year, we here adapt $D_N=2.0$ cm per year for the western portion of this plate to interact with Pacific Plate. And then, the net horizontal force calculated for North American continent should be $F_N=\sim2.4227*10^{17}$ N. To drive North American Plate to move, the net horizontal force F_N needs to overcome the total resistive force, which is mainly consisted of the push force from Pacific Plate and the shearing force from South American Plate. As the push force and the shearing force derive from the basal friction exerted by the asthenosphere, and refer to the

basal friction expression $F_A=\mu Au/y$, the push force provided by Pacific Plate can be written as $F_{PN}= F_N S_P/(S_P+S_N)=1.0261*10^{17}$ N, where S_P and S_N are respectively the area of Pacific Plate and South American Plate. Refer to Table 2, the total resistive force for Australian plate is $F_{Au\text{-}resistive}=3.8640*10^{17}$ N, given 25% of this resistive force is expended to overcome the push force from Pacific Plate, and then, the push force is calculated as $F_{PA}=9.6600*10^{16}$ N. Australian Plate moves dominantly in a northeast direction, the inclination of this direction to latitude (+) is about 76.7^o, as listed in Table 3. Most of North American Plate moves roughly in a southwest direction away from the Mid-Atlantic Ridge, we here assume the push force from North American Plate to be arranged in a southwest direction, the inclination of this direction to latitude (+) is about 190°. Subsequently, the net horizontal force obtained by Pacific Plate can be expressed as $F_P=((F_{PN}^2+F_{PA}^2-2*F_{PN}*F_{PA}*\cos(\alpha-\beta))^{0.5}$, and $\cos\gamma=(F_P^2+F_{PN}^2-F_{PA}^2)/(2*F_P*F_{PN})$, where $\alpha=76.7^o$, $\beta=10^o$. Finally, it is calculated as $F_P=1.096315*10^{17}$ N, and $\gamma=54.03^o$. Similarly, we assume that a majority of the net horizontal force obtained by Pacific Plate has been expended to overcome the total resistive force, which is mainly consisted of the friction exerted by the asthenosphere along Pacific Plate's base. Refer to Table 2, the ratio of the total resistive force and the net horizontal force for South American continent may reach up to 0.99999907. This amplitude allows us to consider a ratio of 0.99999 for Pacific Plate, and then, the total resistive force for Pacific Plate would be $F_{Pa\text{-}resistive}=1.096304*10^{17}$ N. The continental crust's thickness is given as 6.0 km, and refer to Table 1, the average of ocean depth is less than 4.0 km, these two allow us to accept a thickness of 2.0 km to be left for the continental crust to contact the oceanic crust. Pacific Plate's mass may be written as $M_{Pacific}=Sd\rho_{plate}$ (where S, d, and ρ_{plate} are respectively the plate's area, thickness, and density). If we consider the continent's density is the same as the plate's density, and adapt Pacific Plate's area to be 103,300,000.00 km^2, and then, there would be $M_{Pacific}=6.4046*10^{20}$ kg. Applied by equation (2) and given a time of 1,194.45 seconds to accelerate, Pacific Plate finally obtains a movement of 89.44 mm per year, roughly along a northwest direction.

North American Plate presently rotates in a manner of counter clockwise, if we date back, it must had rotated much during a timescale of more than millions of years. It is likely that in the past the push force F_{PN} didn't exist and Pacific Plate was pushed by Australian Plate alone to move along a northeast direction. This sequence implies an abrupt change in motion for Pacific Plate to occur when North American Plate rotated to a central angle, from which a combination of the two lateral forces mentioned above becomes realized. Such a plate motion change had been supported by the Hawaiian–Emperor bend (Sharp and Clague, 2006; Wessel and Kroenke, 2008).
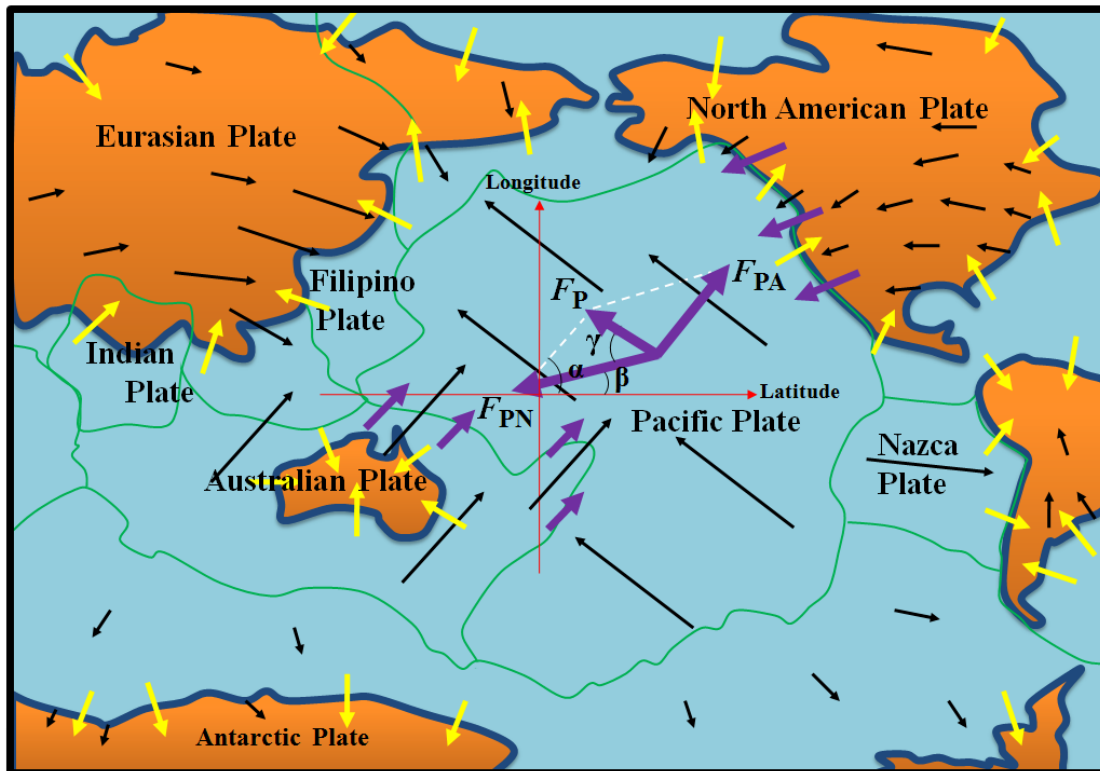
Fig. 7. Modelling the dynamics of Pacific Plate. Black, yellow, and purple arrows denote respectively plate motions, the horizontal forces generated due to oceans, and lateral push forces from related plates. Note that lateral push force $F_{PN}(F_{PA})$ is approximately parallel to the motion of North American (Australian) Plate.

3 Discussion

3.1 Comparison of the ocean-generating force and ridge push

Tectonic stresses are caused by the forces that drive plate tectonics (Middleton and Wilcock, 1996) and may be good experimental field to differentiate the ocean-generating force from ridge push. Figure 8 outlines a vertical distribution of the ocean-generating force and the existing driving forces around North America Plate. It can be found that the region exerted by ridge push on the plate is geographically lower than the regions exerted by the ocean-generating force. As the plate is more rigid, it may be expected that the stresses yielded by a combination of ridge push and collisional resistance would concentrate on the middle and lower part of the plate, whereas the stress yielded by the ocean-generating forces would concentrate on the upper part of the plate. Tectonic stress measurements showed that the stresses manifested concentrate mainly on the uppermost brittle part of the lithosphere, the intraplate and midplate regions are dominated by compression (thrust and strike-slip stress regimes) in which the maximum principal stress is horizontal, and that the maximum horizontal stress direction (Sh Max) keeps parallel to the absolute plate motion (Forsyth &

Uyeda, 1975; Bott and Kusznir, 1984; Zoback et al., 1989; Zoback & Magee, 1991; Zoback, 1992). These results trend to accept the ocean-generating force rather than ridge push as the primary plate driving force. Subsequently, a detailed analysis of stress measurement data found that S_{Hmax} orientations are often rotated into a plane approximately parallel to the local trend of the continental slope (Zoback et al., 1989; Zoback, 1992). As ridge push is geographically lower and its direction is relatively fixed, it is very difficult for this force to create stress field to associate with the continental slope. In contrast, the ocean-generating force is always vertical to the continental slope, it is natural for this force to create stress field to associate with the continental slope.
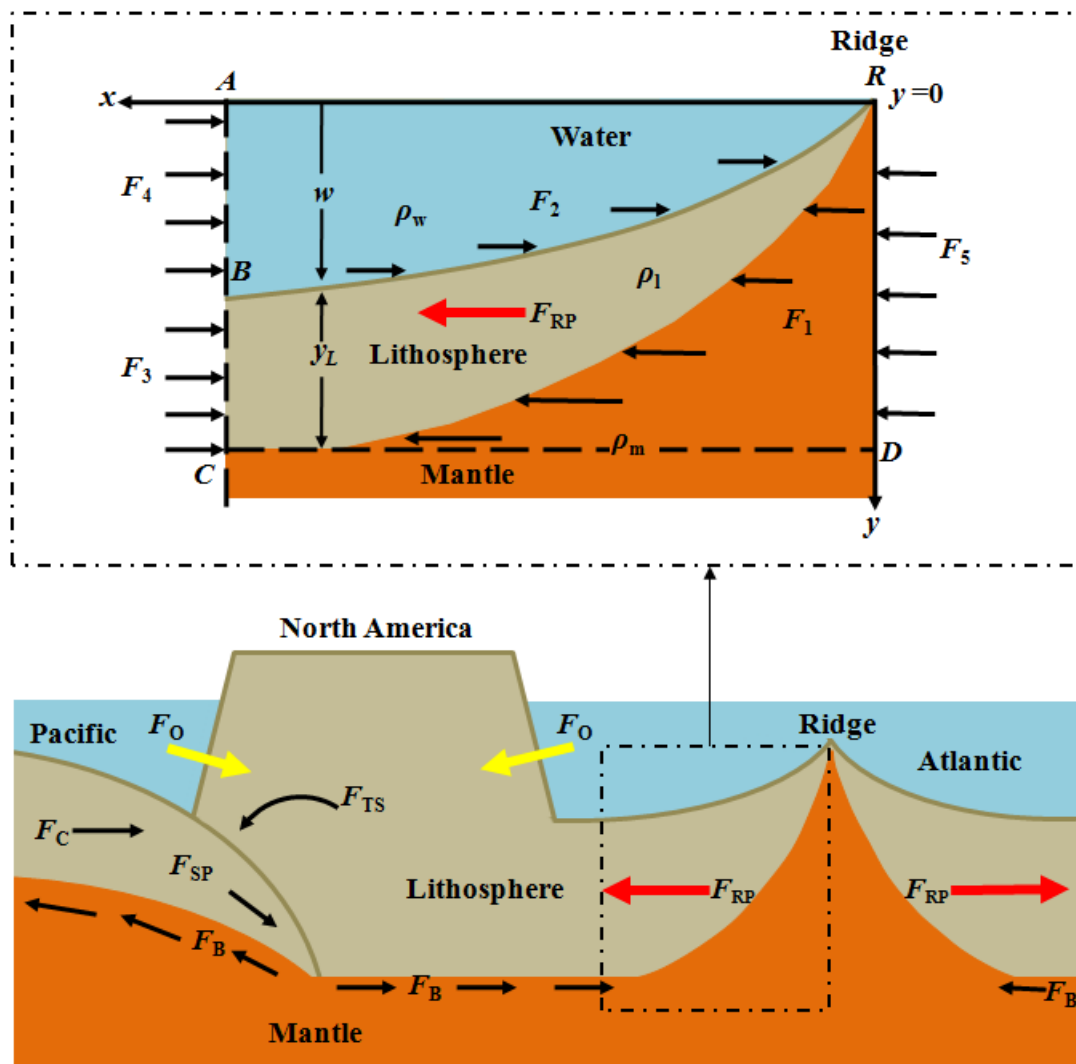
Fig. 8. A distribution of the ocean-generating force and the existed driving forces and a analytic frame for ridge push. F_O, F_{RP}, F_C, F_{TS}, F_{SP}, and F_B denote respectively the horizontal force, ridge push force, collisional resistance, trench suction, slab pull, and basal drag (if resistive). The analytic frame for ridge push refers to Turcotte and Schubert (2014).

According to Turcotte and Schubert (2014), the push force yielded by a ridge may be written as $F_{RP}=g\rho_m\alpha_v(T_1-T_0)(1+2\rho_m\alpha_v(T_1-T_0)/(\pi(\rho_m-\rho_w)))kt$, where g, ρ_m, ρ_w, T_1, T_0, and t are respectively gravitational constant, mantle density, water density, mantle temperature, temperature at plate surface, and age of oceanic plate. This expression requires that, as the density and temperature of mantle increase with depth, the stress yielded by ridge push on the lithosphere would increasingly increase with depth. Contrary to this expectation, the overall trend of decrease in stress was widely established. For instance, the stresses (deviatoric stresses) measured in the upper part of the intraplates hold a magnitude of 20~30 MPa (Forsyth & Uyeda, 1975; Bott and Kusznir, 1984; Zoback & Magee, 1991). At a depth of 50~60 km from ground, the stresses measured at a place beneath the continent's extensional region decrease to almost 8.0 MPa. While at a depth of 100~200 km where it is the lower part of the continental crust, the stresses generally decrease to 15~5 MPa (Mercier, 1980; England and Molnar, 1991).

In fact, even if we agree ridge push to create stress field to cross over the uppermost part of the lithosphere, there still are many challenges for this force. First of all, a single distribution of ridge push is difficult to match the various styles of observed stress fields around the globe. The first release of plate-scale stress fields in the World Stress Map (WSM) database revealed that much of central and northeastern Australia exhibits a NNE compressional stress field, whereas southeastern and southwestern Australia exhibits an E-W compressional stress field, and that the stress field in the midplate North American is uniform over roughly 5000 km in both an E-W direction and a N-S direction (Hiller, 1991; Choy and Bowman, 1990; Zoback, 1992). The ridge at the south of Australian plate is approximately latitudinal, the push force from this ridge may combine collisional resistance at the front of the moving plate to create a NNE compressional stress field, but it is difficult for this ridge to provide a force to create an E-W compressional stress field. Similarly, the ridge at the middle and north Atlantic is approximately longitudinal, the push force from this ridge may create an E-W compressional stress field, but it is difficult for this ridge to provide a force to create a N-S compressional stress field. The subsequent releases of stress fields in the World Stress Map (WSM) database showed that the regional and local patterns of stress fields are complicated and diverse, and cannot be controlled by ridge push (e.g., Sperner, et al., 2003; Heidbach, et al., 2007). Second, the oceanic ridge is geographically far away from the continental crust, usually with a horizontal distance of a few thousands of kilometers, the transition of ridge push from the oceanic crust to the continental crust is still an open question. According to Zoback (1992), the methods of stress measurement involve in earthquake focal mechanisms, well bore breakouts, in situ stress measurements, and young geologic data. Of these, the most reliable are well bore breakouts and in situ stress measurements that were operated in the upper part of

the continental crust. These aspects determine what the observed stresses represent is mainly a status of the upper part of the continental crust. Subsequently, it is rather difficult to imagine how a further and lower ridge push may create stress field to dominate over the upper part of the continental crust. Last, both the knowledge of fluid mechanics and ocean bottom pressure measurement confirm that ocean pressures dominate ocean basins everywhere. As ocean floor is not absolutely flat, ocean pressure creates not only vertically compressional stress but also horizontally compressional stress for the oceanic crust, at the same time ridge push also creates horizontally compressional stress for the oceanic crust, as a result, it is difficult to differentiate the stress yielded by ridge push on the oceanic crust from the stress yielded by ocean pressure.

In contrast, the answer is clear and simple, the ocean-generating forces (i.e., the horizontal forces) may be competent for creating various stress fields to match these observed results. For instance, according to Figure 5 and 6, the ocean-generating forces commonly compress Australian continent inwards, together with an aid from the collisional resistance at the front of the moving plate, a NNE stress field in the central and northeastern Australia and an E-W stress field in the southeastern and southwestern Australia can be formed. Similarly, the generally inward compression yielded by the ocean-generating forces may create an E-W compressional stress field and a N-S compressional stress field for the midplate North American. Geometrically, the ocean-generating forces are always vertical to the continental slopes, the continental slopes own various inclinations from one place to another and usually follow the shapes of coastlines, these features determine that the stress fields yielded by the ocean-generating forces must be diverse. The presently complicated patterns of regional and local stress fields in the intraplates are ascribed mainly to lithospheric properties such as flexure, lateral density contrast, basin geometry, active faulting, and so on (Heidbach, at al., 2007; Heidbach, at al., 2010). We believe, the ocean-generating force plays an important role in controlling the formation of these stress patterns. Additionally, the pressure exerted by ocean on a continental slope may be approximately written as $P = 0.5g\rho_w h$, where g, ρ_w, and h are respectively gravitational constant, water density, and ocean depth. Given g = 10 m/s, ρ_w=1000 kg/m^3, and h = 5 km, the resultant pressure would be P = 25 MPa. This result matches well with the stresses measured in the upper part of the intraplates.

3.2 Formation of Mid-ocean ridge

The travelling continent drags the oceanic crust it connects in the rear, this would yield strain for the latter. We believe, a periodically fracture of the oceanic crust might have been responsible for the formation of MOR. As conceptually outlined in Figure 9, the continent continues to move, the accumulated strain eventually rip the oceanic crust, this allows magma to erupt. The raised magma after cooling crystallizes and creates new crusts. The newly

formed crusts may help seal the fracture and terminate that eruption. The fracture temporarily relieves the accumulated strain, but since the continent continues to move, the strain is again accumulated, the subsequent fracture and closeness occur again. The newly formed crusts add height to the previous oceanic crust, forming the MOR. The representative of this type of MOR may be the Middle-Atlantic Ridge. Of course, not all the MORs are made through this way. For example, the travelling continent would also shear the oceanic crusts respectively at the far and near sides, these shearings may cause these crusts to fracture and form the MORs.
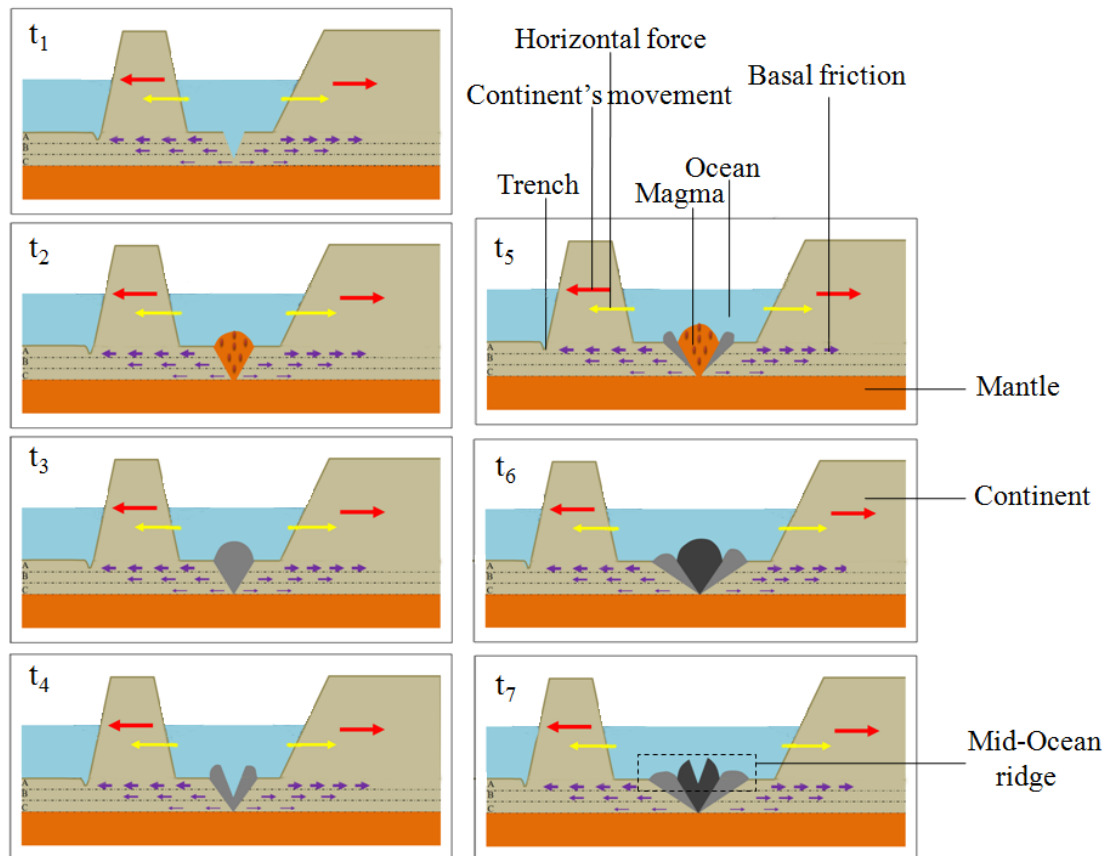
Fig. 9. Modelling the formation of MOR under the ocean-generating forces. From t_1, t_2, ..., to t_7, it exhibits a sequence of forming MOR. The lower lithosphere is apparently divided into three layers A, B, and C, so as to depict different motions due to the drag exerted by basal friction.

3.3 Building of mountains

The travelling continent, if meet another continent in the front, would create high mountain. For example, refer to Figure 10, the horizontal force generated pushes Indian continent to impinge into Eurasian continent, as this force is almost vertical to the continental slope, a bulldozer effect is provided to uplift the materials in the front, forming the Himalayas. It is important to note that, the Himalayas was long thought to be a result of the collision of Indian Plate and Eurasian Plate. This understanding, however, is not exactly correct. The two plates

have same rock density, the collision between them would result in an addition of height. The thickness of the continental (oceanic) crust is about 35 (6) km (Turcotte & Schubert 2002), an overlay of these two plates would form a thickness of at least 70 km, in spite of the folded situation generated for plate itself. Unfortunately, the present-day Himalayas (Mount Everest, 8,848 m) is still too low to reach the requisite height. Instead, if we ascribe the Himalayas to be a result of the collision of two continents, it seems to be practicable. Both the Arabian Sea and Bay of Bengal hold a depth of about 4,000 m, it is this depth to yield the ocean-generating force. Indian continent holds a height of no more 500 m, Tibetan Plateau holds a height of about 4,000~5,000 m, if we add a continent of thickness 4,000 m, which is the same as the sea depth that yields the horizontal force, onto Tibetan Plateau, if material density keeps constant, the requisite height may be obtained. Actually, the Himalayas may provide reference for us to believe that the Alps could have derived from a collision of Italian island and its adjacent Europe. A major reason is the relatively deeper Ionian and Tyrrhenian seas can provide a dominantly lateral push (i.e., the horizontal force) to Italian island. Of course, not all the mountains are made through this way. For instance, most of continents are circled by oceans, the horizontal forces generated would compress all the sides of a continent inwards, these actions deform the continent to create folded mountains.
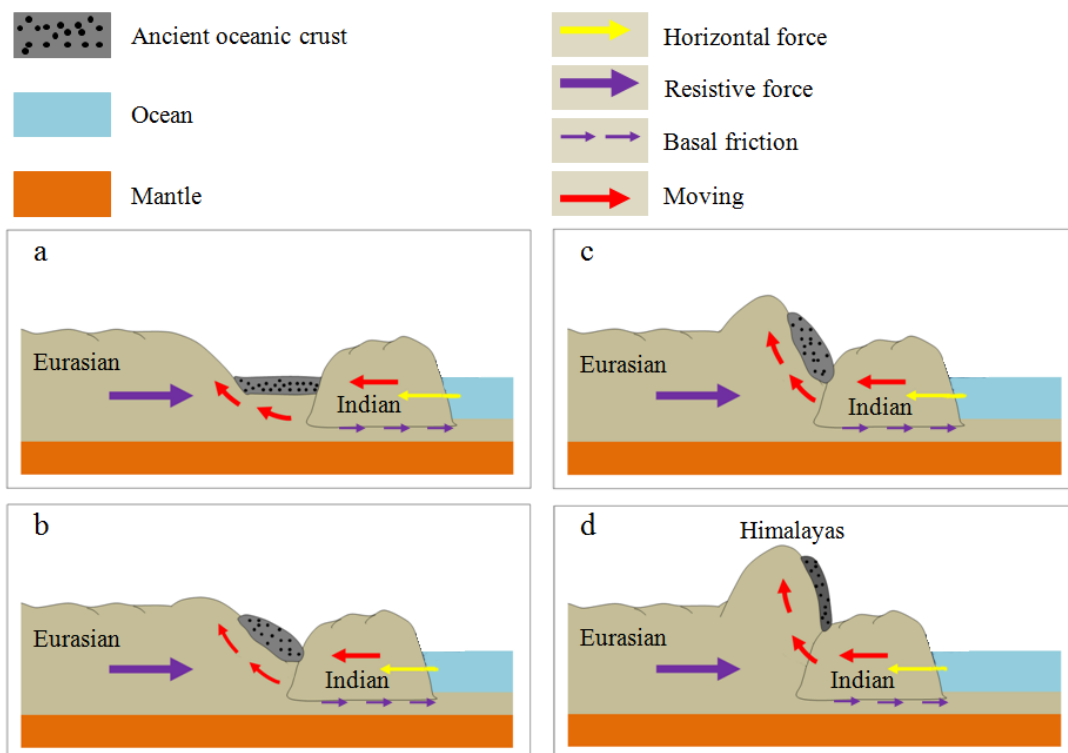

Fig. 10. Modelling the formation of the Himalayas under the collision of Indian continent and Eurasian continent. From a, b, …, to d, it shows a sequence of forming the mountain.

3.4 Creation of transform faults

One of the most unusual features around the MOR is the transform faults which cut the ridge into a train of smaller sections, but the formation of these structures remains poorly understood (Gerya, 2012). The currently accepted view believes that the oceanic transform faults originated from plate fragmentation that is related to pre-existing structures (Wilson, 1965; Oldenburg and Brune, 1972; Cochran and Martinez, 1988; McClay and Khalil, 1998; Choi et at., 2008). Gerya (2010) recently theorized the transform fault of Mid-Atlantic Ridge. A distinguishable feature for the faults is there are many long and nearly-parallel structures that usually cross the ridge to exert the cutting, this suggests that the formation of the ridge is most possibly later than that of these structures. We here consider a solution for the transform faults of the Mid-Atlantic Ridge. As exhibited in Figure 11, the early Atlantic was relatively narrow, the horizontal forces generated continued to push the two continents to move away, the travelling continents in turn dragged the oceanic crusts they connect to, the increasingly accumulated strains eventually split the oceanic crust into smaller nearly-parallel segments. This way of nearly-parallel fracture benefits from the horizontal forces. As these horizontal forces always exert orthogonal to the continents' sides, subsequently, a large number of radial strains are yielded to across the oceanic crust. For each of these nearly-parallel segments, the leading drag to it is along nearly opposed direction, it is mostly possible for the accumulated strain to split the segment in the middle. The fracture, as demonstrated in Figure 9, may yield a ridge. Finally, a segment yields a ridge, a connection of the ridges of all the segments apparently creates the transform faults of the Mid-Atlantic Ridge.
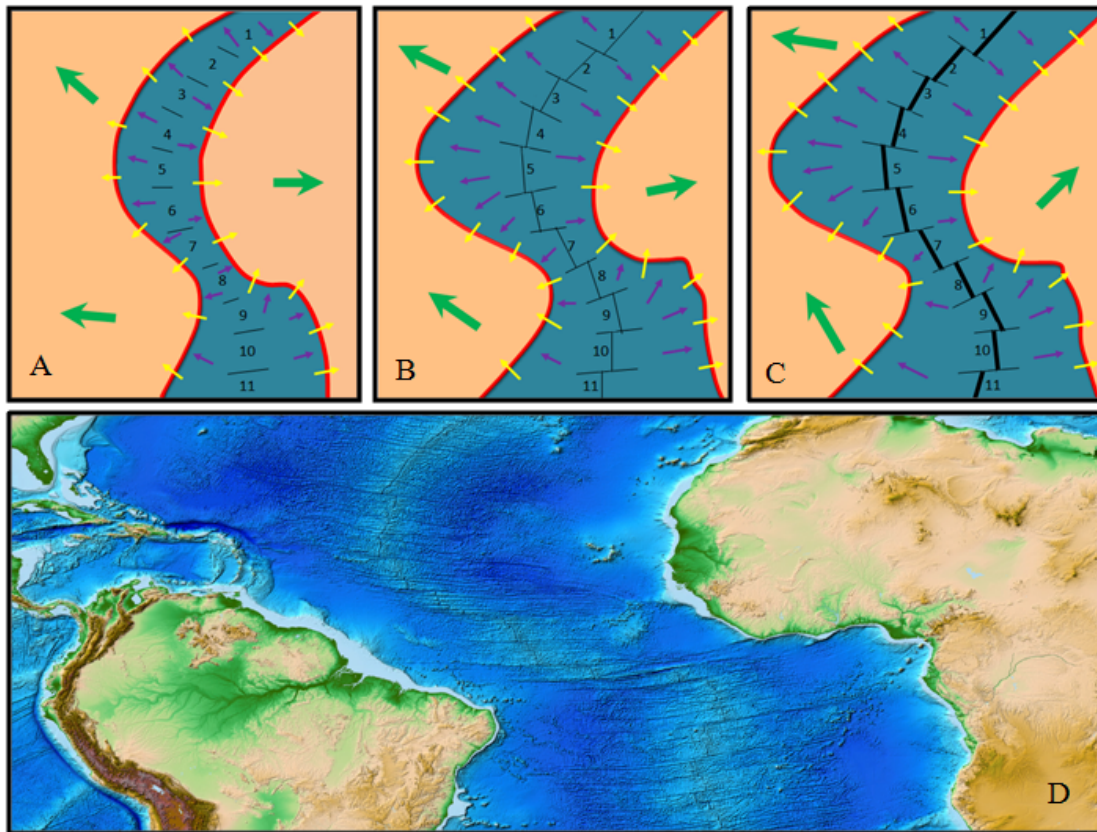
Fig. 11. Modelling the formation of MOR and transform faults. A, B, and C demonstrate a sequence of how transform faults develop with the growth of the MOR. Yellow, green, and purple arrows denote respectively the horizontal forces generated, the resultant movements, and the drags exerted by the travelling continents onto the oceanic crust. The thin black lines represent nearly-parallel structures. Number 1, 2, . . ., and 11 represent the fragments of the oceanic crust, which consist of the sections of transform faults. D shows observed transform faults over the Mid-Atlantic Ridge. The background map is produced from ETOPO1 Global Relief Model (Amante and Eakins, 2009).

3.5 Dispersal of supercontinent

The ocean-generating force driving mechanism provides line for us to conceptually track the dispersal of a supercontinent. Refer to Figure 12, at the time of upper carboniferous the opening at the east of landmass allowed a large body of water to enter, the horizontal force generated pushed the landmass at the two sides of the opening to move away. This separation helped to expand the opening further. With the passage of time, the landmass was gradually separated and displayed the shape at the time of Eocene. This, again, allowed more water to enter, and also more horizontal force to be generated. We speculate, such a positive feedback may have controlled the landmass's initial dispersal. The landmass was nearly broken into pieces at the time of the older quaternary, a relatively primitive layout of separated smaller

continents was formally established. After that, the horizontal force continued to push these continents to move away from each other until present.
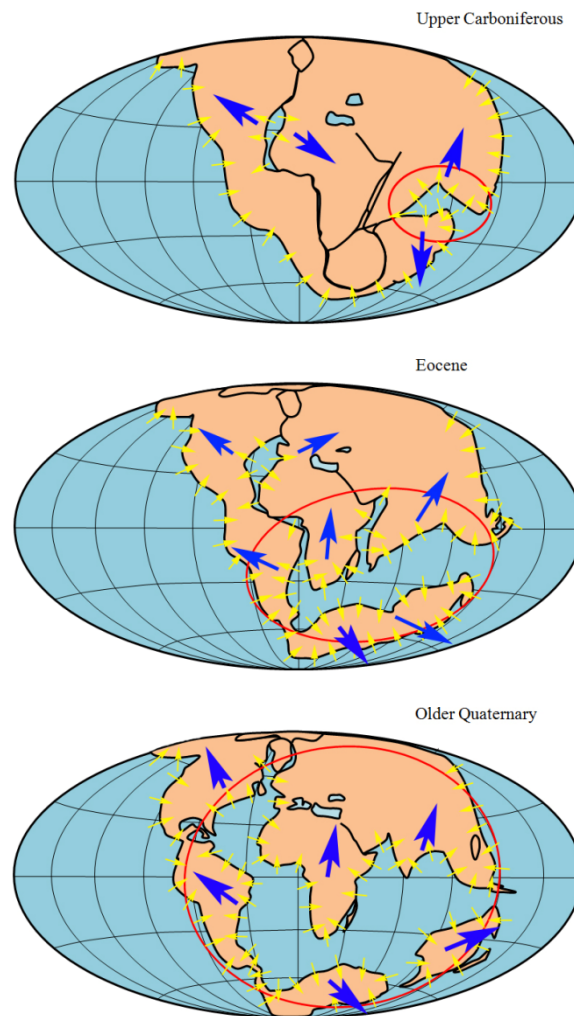

Fig. 12. Modelling the dispersal of supercontinent. Yellow and blue arrows denote respectively the horizontal forces generated due to oceans and the resultant movements. Red circles represent an expansion of the ocean among the landmasses. The background map is yielded referring to Wegener's work (1924).

3.6 Significance of ocean

Water is undoubtedly of great importance for understanding terrestrial phenomena. About 71% the Earth's surface is covered with oceans. It is true, facing such a gigantic body of water, we cannot refuse to consider a coupling of the ocean-generating force and plate motion. Many people feel extraordinarily perplexed why the Earth has plate tectonics but her twin Venus does not. A large number of works showed that water provides right conditions (maintaining a cool surface, for instance) for the Earth's plate tectonics, while the loss of water on the Venus prohibits plate formation (Hilairet et al., 2007; Korenaga, 2007; Lenardic and Kaula, 1994;

Tozer, 1985; Hirth and Kohlstedt, 1996; Lenardic et al., 2008; Landuyt and Bercovici, 2009; Driscoll and Bercovici, 2013). This work extends these understandings, no water on the Venus, no the ocean-generating force, naturally, no formation of plate tectonics on the planet.

References

Amante, C. and Eakins, B.W. (2009). ETOPO1 1 Arc-Minute Global Relief Model: Procedures, Data Sources and Analysis. NOAA Technical Memorandum NESDIS NGDC-24. National Geophysical Data Center, NOAA. doi:10.7289/V5C8276M.

Backus, G., Park, J. & Garbasz, D. (1981). On the relative importance of the driving forces of plate motion. Geophys. J. R. astr. Soc., 67,415-435.

Bercovici, D. (1993). A simple model of plate generation from mantle flow. Geophysical Journal International, 114, 635-650.

Bercovici, D. (1995b). A source-sink model of the generation of plate tectonics from non-Newtonian mantle flow. Journal of Geophysical Research, 100, 2013-2030.

Bercovici, D., Tackeley, P. J., and Ricard, Y. (2015). The generation of plate tectonics from mantle dynamics. Reference Module in Earth Systems and Environmental Science: Treatise on Geophysics (Second Edition), 7, 271-318.

Bokelmann, G. H. R. (2002). Which forces drive North America? Geology, 30(11), 1027-1030.

Bott, M. H. P. (1993). Modeling the Plate-Driving Mechanism. Journal of the Geological Society, 150, 941-951.

Bott, M. H. P. Kusznir, N. J. (1984). The origin of tectonic stress in the lithosphere. Tectonophysics,1984,105, 1-13.

Burchfiel, B. C., et al. (1992). The south Tibetan detachment system, Himalayan Orogeny: extension contemporaneous with and parallel to shortening in a collisional mountain belt. Special Paper, Geological Society of America, 269, 41.

Cadek, O., Ricard, Y., Martinec, Z., and Matyska, C. (1993). Comparison between Newtonian and non-Newtonian flow driven by internal loads. Geophysical Journal International, 112, 103-114.

Cande, S. C., et al. (1989). Magnetic lineations of the world's ocean basins .Tulsa, Oklahoma: American Association of Petroleum Geologists.

Cande, S. C., Kent, D. V. (1992). A new geomagnetic polarity time scale for the Late Cretaceous and Cenozoic. Journal Geophysical Research, 97(10),13917-13951.

Caldwell, P. C., Merrfield, M. A., Thompson, P. R. (2015). Sea level measured by tide gauges from global oceans — the Joint Archive for Sea Level holdings (NCEI Accession 0019568), Version 5.5, NOAA National Centers for Environmental Information, Dataset, doi:10.7289/V5V40S7W.

Cathies, L. (1971). The viscosity of the Earth's mantle, Ph.D. thesis, Princeton Univ., Princeton, N.J.

Choi, E., Lavier, L., Gurnis, M. (2008). Thermomechanics of mid-ocean ridge segmentation. Phys. Earth Planet. Inter., 171, 374-386.

Choy, G. L., and Bowman, J. R. (1990). Rupture process of a multiple main shock sequence: Analysis of teleseismic, local, and field observations of the Tennant Creek, Australia, Earthquakes of January 22, 1988. J. Geophys. Res., 95, 6867-6882.

Christensen, U., Harder, H. (1991). Three-dimensional convection with variable viscosity. Geophysical Journal International, 104, 213-226.

Cochran, J. R., Martinez, F. (1988). Evidence from the northern Red Sea on the transition from continental to oceanic rifting. Tectonophysics, 153, 25-53.

Condiek, C. (2001). Mantle plumes and their record in Earth history. Cambridge, Cambridge University Press, pp 1-306.

Conrad, C. P., Lithgow-Bertelloni, C. (2002). How Mantle Slabs Drive Plate Tectonics. Science, 298 (5591), 207–09.

Conrad, C. P., Lithgow-Bertelloni, C. (2004). The temporal evolution of plate driving forces: Importance of "slab suction" versus "slab pull" during the Cenozoic. J. Geophys. Res., 109, B10407, DOI:10.1029/2004JB002991.

Crameri, F., Conrad, C. P., Montési, L., Lithgow-Bertelloni, C. R. (2018). The dynamic life of an oceanic plate. Tectonophysics. DOI: 10.1016/j.tecto.2018.03.016.

Davies, G. F., and Richards, M. A. (1992). Mantle convection. Journal of Geology. 100, 151-206.

Doglioni, C. (1990). The global tectonic pattern. Journal of Geodynamics, 12, 21-38.

Domeier, M., Torsvik, T. H. (2014). Plate tectonics in the Late Paleozoic.Geoscience Frontiers, 5(3):303-350.

Driscoll, P. and Bercovic, D. (2013). Divergent evolution of Earth and Venus: Influence of degassing, tectonics, and magnetic fields. Icarus. 226, 1447-1464.

Eagles, G. & Wibisono, A. D. (2013). Ridge push, mantle plumes and the speed of the Indian plate. Geophys. J. Int., 194, 670-677.

England, P., Molnar, P. (1991). Inferences of deviation stress in actively deforming belts from simple physical models. Philosophical Transactions of the Royal Society, London, A337, 151-164.

Elsasser, W. M. (1971). Sea-floor spreading as thermal convection, J. geophys. Res., 76, 1101-1112.

Faccenna, C., Bercker, T. W., Lallemand, S., Steinberger, B. (2012). On the role of slab pull in the Cenozoic motion of the Pacific plate. Geophysical research letter, Vol. 39, L03305, doi:10.1029/2011GL050155.

Forsyth, D. & Uyeda, S. (1975). On the relative importance of the driving forces of plate motion. Geophys. J. Int., 43, 163-200.

Foulger, G. R., et, al. (2001). Seismic tomography shows that upwelling beneath Iceland is confined to the upper mantle. Geophys. J. Int., 146, 504-530.

Gerya, T. (2010). Dynamical Instability Produces Transform Faults at Mid-Ocean Ridges. Science, 329, 1047–1050.

Gerya, T. (2012). Origin and models of oceanic transform faults. Tectonophysics, 522-523, 34-54.

Gripp, A. E., and Gordon, R.G. (2002). Young tracks of hot spots and current plate velocities. Geophysical Journal International, 150, 321-361.

Hager, B. H., and O'Connel, R. (1981). A simple global model of plate dynamics and mantle convection. Journal of Geophysical Research. 86, 4843-4867.

Hager, B. H., and Richards, M. A. (1989). Long-wavelength variations in Earth's geoid: Physical models and dynamical implications. Philosophical Transactions of the Royal Society of London, Series A, 328, 309-327.

Hales, A. (1936). Convection currents in the Earth. Monthly Notice of the Royal Astronomical Society, Geophysical Supplement, 3, 372-379.

Heidbach, O., et al. (2018). The World Stress Map database release 2016: Crustal stress pattern across scales. Tectonophysics, 744,484-498.

Heidbach, O., Rajabi, M., Reiter, K. Ziegler, M., and the WSM Team. (2016). World Stress Map Database Release 2016, GFZ Data Services.

Heidbach, O., et al. (2007). Plate boundary forces are not enough: Second- and third-order stress patterns highlighted in the World Stress Map database, Tectonics, 26, http://doi.org/10.1029/2007TC002133 (PDF).

Heidbach, O., et al. (2010). Global crustal stress pattern based on the World Stress Map database release 2008. Tectonophys, 482, 3-15.

Hess, H. H. (1962). History Of Ocean Basins, in Engel, A. E. J., James, H. L., & Leonard, B. F., eds. Petrologic Studies: A volume in honor of A. F. Buddington. Boulder, CO, Geological Society of America, 599-620.

Hibsch, C., et al. (1995). Paleostress analysis, a contribution to the understanding of basin tectonics and geodynamic evolution: example of the permian-cenozoic tectonics of Great Britain and geodynamic implications in Western Europe. Tectonophysics, 252, 103-136.

Hilairet, N., Reynard, B., Wang, Y., et al. (2007). High-pressure creep of serpentine, interseismic deformation, and initiation of subduction. Science, 318(5858), 1910-1913.

Hiller, R. (1991). Australia-Banda arc collision and in situ stress in the Vulcan suh-basin (Timor Sea) as revealed by borehole breakout data. Exp. Geophys., 22, 189-194.

Hirth, G. and Kohlstedt, D. (1996). Water in the oceanic upper mantle: Implications for rheology, melt extraction and the evolution of the lithosphere. Earth and Planetary Science Letters, 144, 93-108.

Holmes, A. (1931). Radioactivity and Earth Movements. Nature, 128, 496-496.

James, T. S., Gowan, E. J., Wada, L., and Wang, K. L. (2009). Viscosity of the asthenosphere from glacial isostatic adjustment and subduction dynamics at the northern Cascadia subduction zone, British Columbia, Canada. Journal of Geophysical Research: Solid Earth,114(B4), CiteID B04405.

Jeffreys, H. (1929). The Earth,2 nde d., p. 304, Cambridge University Press, London.

Jordan, T. H. (1974). Some comments on tidal drag as a mechanism for driving plate motions. J. Geophys. Res., 79, 2141-2142.

King, S. D. (1995). The viscosity structure of the mantle. In Reviews of Geophysics (Supplement) U.S. Quadrennial Report to the IUGG 1991-1994, 11-17.

Knopoff, L., and Leeds, A. (1972). Lithospheric momenta and the deceleration of the Earth. Nature, 237, 93-95.

Korenaga, J. (2007). Thermal cracking and the deep hydration of oceanic lithosphere: A key to the generation of plate tectonics? Journal of Geophysical Research 112(B5), DOI: 10.1029/2006JB004502.

Landuyt, W. and Bercovici, D. (2009). Variations in planetary convection via the effect of climate on damage. Earth and Planetary Science Letter, 277, 29-37.

Lay, T. (1994). The fate of descending slabs. Annual Review of Earth and Planetary Sciences. 22, 33-61.

Lenardic, A., Jellinek, M., and Moresi, L-N. (2008). A climate change induced transition in the tectonic style of a terrestrial planet. Earth and Planetary Science Letters, 271, 34-42.

Lenardic, A. and Kaula, W. (1994). Self-lubricated mantle convection: Two-dimensional models. Geophysical Research Letters, 21, 1707-1710.

Ma, Z. J., Li, C. D., Gao, X. L. (1996). General characteristics of global tectonics in the Mesozoic and Cenozoic (in Chinese). Geological Science and Technology Information, 15(4), 21-25.

Mallard, C., et al. (2016). Subduction controls the distribution and fragmentation of Earth's tectonic plates. Nature, 535 (7610), 140-143.

McClay, K., Khalil, S. (1998). Extensional hard linkages, eastern Gulf of Suez, Egypt. Geology, 26, 563-566.

Mercier, J. C. C. (1980). Magnitude of the continental lithospheric stresses inferred from rheomorphic petrology. Journal geophysical research, B,1980,85(11), 6293-6303.

McKenzie, D. P. (1968). The Influence of the Boundary Conditions and Rotation on Convection in the Earth's Mantle. The Geophysical Journal, 15, 457-500.

McKenzie, D. P. (1969). Speculations on the Consequences and Causes of Plate Motions. The Geophysical Journal,18,1-32.

Middleton, G. V., Wilcock, P. R. (1996). Mechanics in the Earth and Environmental Sciences. Cambridge University Press, Australia : pp 496.

Minster, J. B., Jordan, T. H., Molnar, P., Haines, E. (1974). Numerical modelling of instantaneous plate tectonics. Geophys. J. 36(3), 541-576.

Minster, J. B., Jordan, T. H. (1978). Present-day plate motions. Journal Geophysics Research, 83(10),5331-5354.

Mitrovica, J. X. (1996). Haskell (1935) revisited. Journal of Geophysical Research, 101, 555-569.

Morgan, W. J. (1972). Deep mantle convection plumes and plate motions. Bull. A. Pet. Geol., 56, 203-213.

O'Connell, R., Gable, C. G., and Hager, B. (1991). Toroidal-poloidal partitioning of lithospheric plate motions, in Sabadini, R., et al., eds., Glacial isostasy, sea-level and mantle rheology: Dordrecht, The Netherlands, Kluwer Academic Publisher, 334, 535-551.

Ogawa, M. (2008). Mantle convection: A review. Fluid Dynamics Research. 40, 379-398.

Oldenburg, D. W., Brune, J. N. (1972). Ridge transform fault spreading pattern in freezing wax. Science, 178, 301-304.

Oxburgh, E. and Turcotte, D. (1978). Mechanisms of continental drift. Reports on Progress in Physics, 41, 1249-1312.

Perkeris, C. (1935). Thermal convection in the interior of the Earth. Monthly Notices of the Royal Astronomical Society, Geophysical Supplement, 3, 343-367.

Pugh, D. T. (1987). Tides, Surges and Mean Sea-Level. JOHN WILEY & SONS.

Pugh, D. T. and Woodworth, P. L. (2014). Sea-Level Science: Understanding Tides, Surges Tsunamis and Mean Sea-Level Changes. Cambridge Univ. Press, Cambridge.

Ranalli, G. & Chandler, T. E. (1975). The Stress Field in the Upper Crust as determined from in situ Measurements. - Geol. Rundsch., 64, 653–74.

Read, H. H. & Watson, J. (1975). Introduction to Geology. New York, Halsted, pp13-15.

Richardson, R.M., Cox, B.L. (1984). Evolution of oceanic lithosphere: A driving force study of the Nazca Plate. Journal of Geophysical Research: Solid Earth. 89 (B12), 10043-10052.

Richardson, R. M. (1992). Ridge Forces, Absolute Plate Motions, and the Intraplate Stress Field. Journal of Geophysical Research, 97, 11739-11748.

Richter, F. (1973). Dynamical models for sea-floor spreading, Rev. Geophys. Space Phys., 11, 223-287.

Runcorn, S. (1962a).Towards a theory of continental drift. Nature,193, 311-314.

Runcorn, S. (1962b). Convection currents in the Earth's mantle. Nature, 195, 1248-1249.

Sharp, W. D. and Clague, D. A. (2006). 50-Ma Initiation of Hawaiian–Emperor bend records major change in Pacific plate motion. Science, 313(5791): 1281-1284.

Silver, P. G., Carlson, R. W., and Olson, P. (1988). Deep slabs, geochemical heterogeneity, and the large-scale structure of mantle convection. Annual Review of Earth and Planetary Sciences. 16, 477-541.

Sleep, N. H. & Toksoz, M. N. (1971). Evolution of marginal basins, Nature, 233, 548-550.

Spence, W. (1987). Slab pull and the seismotectonics of subducting lithosphere. Reviews of Geophysics, 25 (1), 55–69.

Sperner, B., et al. (2003). Tectonic stress in the Earth's crust: advances in the World Stress Map project, in New insights in structural interpretation and modelling, edited by D. A. Nieuwland, Special Publication 212, 101-116, Geol. Soc. Spec. Pub., London.

Stein, C., Schmalzl, J., Hansen, U. (2004). The effect of rheological parameters on plate behavior in a self-consistent model of mantle convection. Physics of the Earth and Planetary Interiors, 142, 225-255.

Sykes, L. R. (1967). Mechanism of earthquakes and nature of faulting on the mid-oceanic ridges. J. geophys, Res., 72, 2131-2153.

Tackley, P. (1998). Self-consistent generation of tectonic plates in three-dimensional mantle convection. Earth and Planetary Science Letters, 157, 9-22.

Tanimoto, T., Lay, T. (2000). Mantle dynamics and seismic tomography. Proceedings of the National Academy of Sciences, 97 (23),12409–12410.

Torsvik, T. H. et al., (2008) Global plate motion frames: toward a unified model. Review Geophysics, 46, RG3004.DOI:10.1029/2007RG000227.

Tozer, D. (1985). Heat transfer and planetary evolution. Geophysical Surveys, 7, 213-246.

Trompert, R., Hansen, U. (1998). Mantle convection simulations with reheologies that generate plate-like behavior. Nature, 395, 686-689.

Turcotte, D. L., and Oxburgh, E. (1972). Mantle convection and the new global tectonics. Annual Review of Fluid Mechanics, 4, 33-66.

Turcotte, D. L., Schubet, G. (1982). Geodynamics: applications of continuum physics to geophysical problems. New York: John Wiley & Sons.

Turcotte, D. L., Schubert, G. (2002). Plate Tectonics. Geodynamics (Second Edition). Cambridge University Press. pp.1-21. ISBN: 0-521-66186-2.

Turcotte, D. L., Schubert, G. (2014). Geodynamics (Third Edition). Cambridge University Press, Cambridge. ISBN: 978-0-521-18623-0.

Vigny, C., et al. (1991). The Driving Mechanism of Plate Tectonics. Tectonophysics, 187, 345-360.

Vine, F. J., & Matthews, D. H. (1963). Magnetic Anomalies Over Oceanic Ridges. Nature, 199, 947-949.

Wan, T. F. (1993). Tectonic stress field and its application to the intraplate in Eastern China (in Chinese). Beijing, Geological Publishing Company, pp 1-103.

Wan, T. F. (2018). On the dynamic mechanics of global lithosphere plate tectonics (In Chinese). Earth Science Frontiers, 25, DOI:10.13745/j.esf.sf.2018.1.1.

Wegener, A. (1915). The Origin of Continents and Oceans. New York, NY: Courier Dover Publications.

Wegener, A. (1924). The origin of continents and oceans (Entstehung der Kontinente und Ozeane). Methuen & Co.

Weinstein, S. (1998). The effect of convection planform on the toroidal-poloidal energy ratio. Earth and Planetary Science Letters, 155, 87-95.

Wessel, P. & Kroenke, L.W. (2008). Pacific absolute plate motion since 145 Ma: An assessment of the fixed hot spot hypothesis. Journal of Geophysical Research - Solid Earth 113(B6). http://dx.doi.org/10.1029/2007JB005499.

White, R., McKenzie, D. (1989). Magmatism at rift zones: The generation of volcanic continental margins and flood basalts. Journal of Geophysical Research, 94, 7685-7729.

Wilson, J. T. (1963). A possible origin of the Hawaiian Island. Canada Journal of Physics, 41, 863-868.

Wilson, J. T. (1965). A new class of faults and their bearing on continental drift. Nature, 207, 343-347.

Wilson, J. T., Burke, K. (1973). Plate tectonics and plume mechanics. EOS, Trans. Am. geophys, Un., 54, 238-239.

Zoback, M. L., et al. (1989). Global patterns of tectonic stress. Nature, 341, 291-298.

Zoback, M. L., Magee, M. (1991). Stress magnitudes in the crust: constraints from stress orientation and relative magnitude data. Philosophical Transactions of the Royal Society, London, A337(1645), 181-194.

Zoback, M. L. (1992). First- and Second-Order Patterns of Stress in the Lithosphere:The World Stress Map Project. Journal of geophysical research, 97(B8),11703-11728.